



Review Article

Advances and Emerging Alternatives in Modified Cellulose Nanocrystals for Elastomer Reinforcement: A Review

Muhammad Thoriq Al Fath*

Faculty of Chemical and Process Engineering Technology, Universiti Malaysia Pahang Al-Sultan Abdullah, Lebuh Persiaran Tun Khalil Yaakob, Kuantan, Pahang, Malaysia

Department of Chemical Engineering, Faculty of Engineering, Universitas Sumatera Utara, Padang Bulan, Medan, Indonesia

Khairatun Najwa Mohd Amin

Faculty of Chemical and Process Engineering Technology, Universiti Malaysia Pahang Al-Sultan Abdullah, Lebuh Persiaran Tun Khalil Yaakob, Kuantan, Pahang, Malaysia

* Corresponding author. E-mail: thoriq@usu.ac.id DOI: 10.14416/j.asep.2026.01.010

Received: 18 August 2025; Revised: 19 October 2025; Accepted: 18 November 2025; Published online: 27 January 2026

© 2026 King Mongkut's University of Technology North Bangkok. All Rights Reserved.

Abstract

Cellulose nanocrystals (CNCs) are increasingly recognised as sustainable nanofillers for elastomer composites due to their biodegradability and excellent mechanical properties. However, their inherent hydrophilicity limits compatibility with hydrophobic elastomer matrices, creating significant challenges for effective reinforcement. To overcome this, significant progress has been made through surface modification strategies. Physical approaches such as adsorption and plasma treatment improve compatibility via non-covalent interactions. While chemical routes including etherification/esterification, grafting, silylation, and nucleophilic modification introduce covalent bonds that adapt CNCs surface chemistry to polymer matrices. Such modifications have been shown to reliably improve dispersion, strengthen interfacial adhesion, and enhance both the thermal stability and mechanical performance of elastomer composites when compared with those reinforced by unmodified CNCs. Lignin-containing CNCs (LCNCs) offer distinct advantages by combining inherent hydrophobicity, thermal shielding, and simpler processing, making them a promising bio-based alternative to extensively modified CNCs (M-CNCs). Nonetheless, industrial implementation remains constrained by process complexity, high costs, and performance trade-offs at different filler loadings.

Keywords: Cellulose nanocrystals, Elastomer composites, Lignin-containing CNCs, Modified CNCs, Surface modification

1 Introduction

In recent years, the development of biodegradable and bio-based polymer composites has attracted significant attention due to their potential to replace conventional plastics in sustainable applications. These materials have shown improved printability and dimensional stability in additive manufacturing processes, highlighting the role of nanomaterials in enhancing the mechanical and functional performance of bio-composites [1].

CNCs are a promising type of bio-based nanomaterial, known for their exceptional mechanical strength, biodegradability, high surface area, and renewability. They are commonly derived from natural cellulose sources such as wood pulp, cotton, and bacterial cellulose through processes including acid hydrolysis and enzymatic treatment [2], [3]. CNCs are rigid, rod-like nanomaterials typically obtained via acid hydrolysis or enzymatic treatment of cellulose sources such as wood, cotton, or agricultural residues [4]. The common morphology of CNCs



features diameters ranging from 1 to 100 nm and elongated lengths between 500 and 2000 nm, providing a large surface area, low density, minimal thermal expansion coefficient, small aspect ratio, and high specific strength [5]. These inherent properties enable CNCs to provide effective load transfer, interfacial adhesion, and mechanical reinforcement when well-dispersed in elastomer matrices [6]. Typically, CNCs are fabricated through sequential steps, including biomass pretreatment, delignification, bleaching, and controlled hydrolysis using acids, enzymes, or ionic liquids. These fabrication routes influence the crystallinity, aspect ratio, and surface chemistry of CNCs, which subsequently determine their compatibility and reinforcing performance in elastomer matrices [7]. Owing to their unique crystalline structure, CNCs possess high stiffness and strong reinforcing capabilities, making them highly effective as nanofillers in various polymer systems, including elastomer composites [8], [9].

Elastomers such as polyurethane (PU), thermoplastic polyurethane (TPU), natural rubber (NR), and styrene–butadiene rubber (SBR) are used in applications requiring elasticity, durability, and resilience, from automotive parts to sustainable packaging [10]. While carbon black and silica have traditionally served as reinforcing fillers, sustainability and environmental concerns are driving interest in renewable options like CNCs [2], [11].

The use of CNCs for elastomer reinforcement presents several key challenges that must be addressed to ensure their successful integration and performance in polymer matrices. The first challenge is related to compatibility and dispersion. Because CNCs are highly hydrophilic, they are often poorly compatible with elastomers, which tend to be hydrophobic. This mismatch leads to poor dispersion and weak interfacial bonding between the CNCs and the elastomer matrix [3], [12]. A similar interfacial compatibility issue has been reported in polymer composites, where chemical modification of the epoxy matrix using silane coupling agents significantly improved filler dispersion and adhesion strength, leading to enhanced mechanical performance [13]. Additionally, due to their high surface energy, CNCs tend to form agglomerates, resulting in poor dispersion within elastomer matrices. This aggregation negatively affects the mechanical reinforcement efficiency of CNCs and ultimately diminishes the overall composite performance [9], [10].

The thermal stability of CNCs is also a concern. Although they offer outstanding mechanical strength, they begin to degrade at temperatures above 200 °C. This characteristic hinders their use in elastomeric applications that require high-temperature curing or extrusion processes [3], [10]. The resulting thermal degradation weakens CNC's structural integrity and produces by-products that can hinder polymerization and reduce elastomer matrix stability [11].

Another problem involves mechanical and barrier property issues at higher CNCs loading levels. As the CNCs content increases, the composite may exhibit increased brittleness and reduced flexibility, which contradicts the essential properties of elastomeric materials such as high elasticity and energy dissipation [2], [14]. Thus, it is crucial to achieve an optimal balance between CNCs content and elastomer properties. Similar optimization between filler content and matrix interaction has also been demonstrated in natural fiber/epoxy composites, where controlled fiber loading enhanced tensile, flexural, and viscoelastic properties of the material [7].

This study aims to provide a comprehensive review of CNCs' surface modification strategies for elastomer composites by analyzing keyword co-occurrence to identify research development and trends, reviewing and classifying key physical and chemical modification techniques (including compatibility and dispersion, thermal stability, and mechanical properties), and evaluating LCNCs as an alternative approach to enhance compatibility and reinforcement performance.

2 Methodology

A bibliometric approach was employed to systematically identify, evaluate, and analyze the body of literature related to the modification of CNCs for elastomer composite applications. The Scopus database was selected as the primary data source because of its comprehensive coverage of peer-reviewed journals in materials science, polymer engineering, and nanotechnology. The search process was conducted in April 2025, using the keywords “cellulose nanocrystals,” “CNCs,” “modification,” “surface modification,” and “elastomer composites” combined with Boolean operators (AND/OR) to refine the query. The search was limited to journal articles and reviews published between 2010 and 2025 to capture both foundational and recent advancements in this area.

After applying these criteria, a total of 511 documents were initially retrieved. The search results were exported in Research Information Systems (RIS) format, and metadata such as title, authors, abstract, keywords, year of publication, and citation count were included. Duplicate entries or irrelevant publications were automatically removed at this stage to preserve the integrity of the dataset. A manual screening was then performed by reviewing titles and abstracts to ensure relevance to the topic. Articles written in languages other than English or unrelated to CNCs modification were excluded, reducing the dataset to 506 eligible documents. Full-text access was verified for all remaining publications.

A comprehensive evaluation of the 506 full-text articles was subsequently carried out, resulting in the exclusion of 484 documents that did not directly address CNCs modification for elastomer composites. The final dataset consisted of 22 articles that met the inclusion criteria and formed the basis for the review analysis. These articles were further examined for

details such as fabrication methods involving physical modifications (e.g., surface adsorption and plasma treatment) and chemical modifications (e.g., etherification/esterification, grafting, silylation, and nucleophilic modification).

The bibliometric data were processed and analyzed using Microsoft Excel and Visualization of Similarities Viewer (VOSviewer, version 1.6.20) to visualize publication trends, keyword co-occurrence networks, and citation relationships among the selected studies. This combination of software ensured reproducibility and transparency in the analytical process. The Preferred Reporting Items for Systematic Reviews and Meta-Analyses (PRISMA) flow diagram, presented in Figure 1, summarizes the step-by-step screening and selection process from initial identification to final inclusion, providing a clear and systematic overview of the dataset refinement procedure.

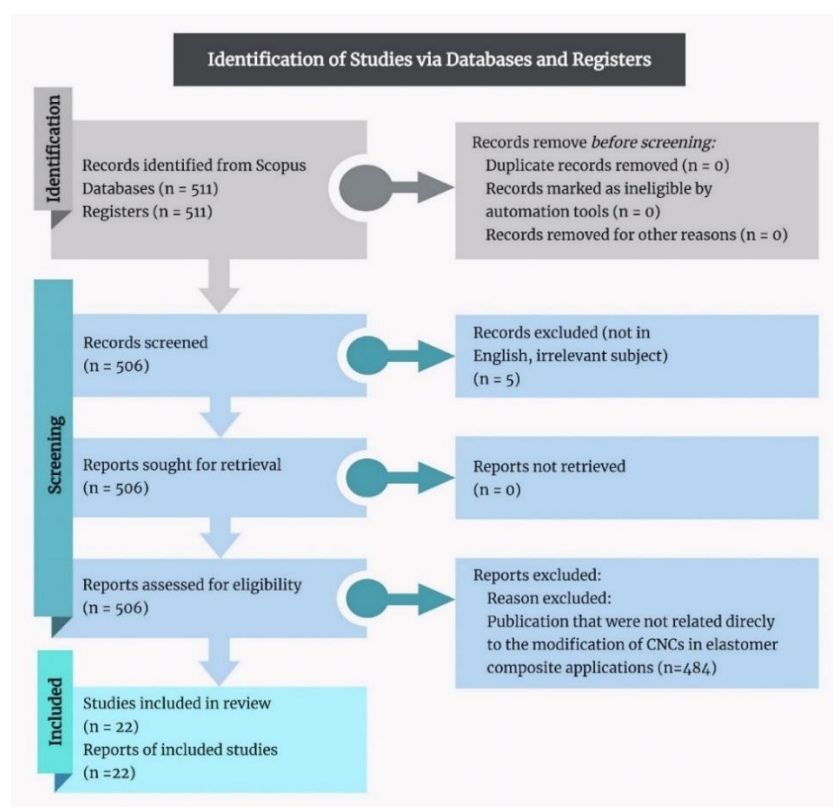


Figure 1: PRISMA flow diagram representing the literature screening and selection process for the review (Adapted from [15]).

3 Results and Discussion

3.1 Keyword co-occurrence analysis

To understand the thematic structure and conceptual evolution of research on CNCs and their derivatives, a keyword co-occurrence analysis was conducted. This bibliometric mapping identifies how frequently

specific terms appear together within scientific publications, providing insight into dominant research areas, active subfields, and underexplored connections. By visualizing these associations, one can observe the intellectual landscape of CNCs research and detect both well-established and emerging directions.

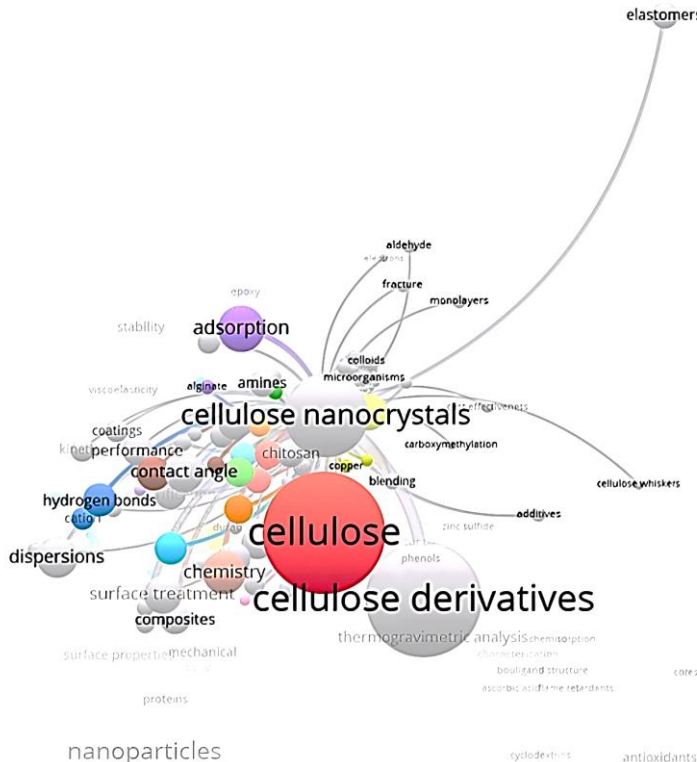


Figure 2: Network visualization of keyword co-occurrence analysis.

Figure 2 illustrates the keyword co-occurrence network in cellulose-based material research, highlighting dominant themes and emerging directions. Core terms such as “cellulose,” “cellulose derivatives,” and “cellulose nanocrystals” reflect the field’s strong foundation in material design and surface functionalization. Surrounding these core terms are active research areas in surface chemistry, indicated by keywords such as “hydrogen bonds” and “adsorption”. Despite these developments, the network also reveals notable gaps. The term “elastomers” appears only at the margins, suggesting that the potential of CNCs in elastomer composites remains underexplored. This represents a missed opportunity given their promise to enhance mechanical performance and sustainability. It can be

inferred that the current research landscape is concentrated on nanostructure design, surface modification, and material processing, while broader applications in elastomers remain inadequately addressed.

3.2 Surface modification strategies for CNCs in elastomer

The bibliometric analysis presented in the earlier section reveals a growing academic interest in CNCs research, particularly in relation to their surface chemistry, polymer compatibility, and elastomer applications. However, it also exposes critical gaps, most notably the underexplored potential of CNCs in elastomer systems. To address these gaps, this section

reviews surface modification strategies designed to improve CNCs compatibility with elastomers. It provides an in-depth examination of physical, chemical, and alternative modifications that enable CNCs to function effectively as reinforcing agents in elastomer composites. CNCs possess high mechanical strength, biodegradability, and renewability, making them promising elastomer reinforcements [2], [3], yet their use is limited by interparticle interactions, poor matrix compatibility, and moisture sensitivity that cause aggregation and poor dispersion [3], [9]. Targeted surface modifications are therefore required to enhance polymer interactions and maximize reinforcing potential [11], [12].

Modification strategies for CNCs primarily focus on improving their dispersion, compatibility, and interfacial adhesion in elastomer composites [9], [12]. Physical modifications, including surface adsorption and plasma treatment, enhance CNCs dispersion and improve their processability [3], [8].

The formation of a continuous nanocellulose network within elastomer matrices is governed by the critical percolation threshold, representing the minimum filler concentration required to establish an interconnected stress-bearing structure. For unmodified CNCs, their hydrophilic nature and poor compatibility with nonpolar elastomers result in relatively high percolation thresholds, typically around 5–10 wt%, where aggregation often occurs before a stable reinforcing network can form [3], [9].

Surface modification substantially lowers this threshold by improving dispersion and interfacial adhesion between CNCs and the polymer matrix. For example, plasma-treated CNCs in polyfarnesene exhibit a percolation threshold near 1.5 wt%, reflecting enhanced connectivity and stress transfer [12]. In general, modified CNCs (M-CNCs), such as silylated or grafted forms, form percolating networks at 1–3 wt%, while liquid-crystalline CNCs achieve network formation at even lower loadings (≤ 1 wt%) due to their anisotropic, self-assembled architectures [9], [11], [14]. These observations, consistent with the data summarized in Table 1, indicate that the percolation threshold strongly depends on surface functionality, aspect ratio, and degree of alignment, which together control the balance between reinforcement efficiency and elasticity in CNCs-reinforced elastomer systems.

Chemical modifications, including etherification/esterification, grafting, silylation, and nucleophilic modification, add functional groups that enhance CNCs' polymer interactions [2], [11], [14]. Alternative approaches, such as Lignin-containing CNCs (LCNCs) and their potential for elastomers, provide multifunctionality, ensuring CNCs contribute to the development of high-performance, sustainable elastomer composites [3], [9]. The discussion consists of three main approaches: physical, chemical, and alternative modifications, as summarized in Figure 3.

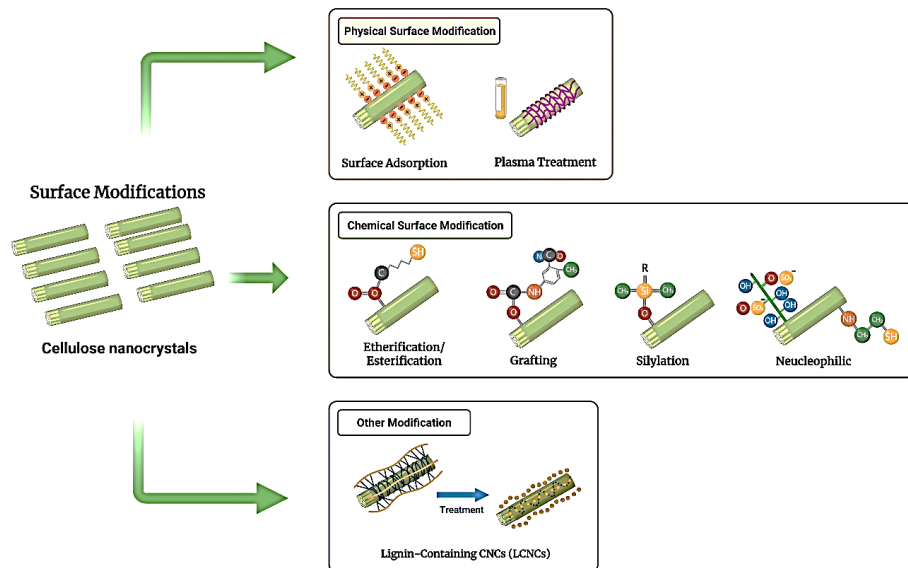


Figure 3: Overview of surface modification strategies for CNCs, including physical, chemical, and LCNCs analysis.

**Table 1:** Final review of data synthesis.

No.	Nanocellulose	Modification	Nanocomposite	Findings	Ref.
1	Commercial 11.5 wt% aqueous CNCs suspension (sulfuric acid hydrolysis)	Physical Modification: Surface Adsorption Tetra decyl trimethyl ammonium bromide (TTAB)	Polystyrene (PS)/CNCs (5 wt%) & PS/M-CNCs (1, 5, 10 wt%)	<ul style="list-style-type: none"> - Unmodified CNCs: Glass transition temperature (Tg) 108 °C, Water Contact Angle (WCA) < 50°, C/O 0.21, early weight loss < 100 °C, SEM showed holes and poor dispersion. - M-CNCs: WCA 97°, carbon-to-oxygen atomic ratio (C/O) 0.50, no weight loss < 100 °C, no SEM holes, improved compatibility. - Plasticization observed at 1–5 wt% with no modulus gain. - 10 wt% gave an increased rubbery modulus, indicating reinforcement. 	[16]
2	Nanocrystalline cellulose (NCC) from Softwood pulp	Physical Modification: Surface Adsorption Cetyltrimethyl ammonium bromide (CTMAB)	Natural Rubber Latex (NRL)/NCC (5 phr) & NR/M-NCC (5, 10, 15, 20 phr)	<ul style="list-style-type: none"> - Unmodified NCC: zeta potential -45.2 mV, crystallinity 72.2%, poor dispersion, weak interaction with NR, low tensile and tear strength. - M-NCC: zeta potential +24.9 mV, CTMAB ~20.2 wt%, crystallinity 69.4%, better dispersion and interface, improved tensile and tear strength. - Best properties at 10 phr: tensile \pm 30.3 MPa (+26%), tear 40.3 kN/m, elongation 670.4%. - Overloading (15–20 phr) caused property decline. 	[17]
3	Commercial CNCs from Celluforce	Physical Modification: Plasma Treatment Plasma-induced polymerization with trans- β -farnesene	Polyfarnesene (PF)/CNCs (0.5 wt%) & PF/M-CNCs (0.5–5.0 wt%).	<ul style="list-style-type: none"> - Unmodified CNCs: hydrophilic, poor compatibility with PF, crystallinity 72.3%, molecular weight (MW) 137 kDa, limited reinforcement. - Plasma-M-CNCs: enhanced hydrophobicity, better dispersion, crystallinity 69.9%, MW up to 2296 kDa, improved storage modulus. - 1.5 wt% identified as percolation threshold with optimal storage modulus (G') and network formation. - High loadings (3–5 wt%) led to viscoelastic tuning but reduced catalytic activity. - TGA revealed M-CNCs had lower moisture loss near 100 °C, with all samples degrading at ~250 °C and ~300 °C, and showing similar thermal stability to CNCs. 	[3]
4	CNCs from linter by sulfuric acid hydrolysis	Chemical Modification: Etherification/Esterification Acetic anhydride	Polyurethane (PU)/CNCs (0 wt%) & PU/Acetylated CNCs (ACNs) (M-CNCs) (5–25 wt%).	<ul style="list-style-type: none"> - Unmodified CNCs: poor dispersion in nonpolar PU, tensile 2.79 MPa, modulus 0.98 MPa, elongation 208%, Tg 14.5 °C. - ACNs: improved dispersion in tetrahydrofuran (THF), reduced polarity, crystalline structure retained, strong interfacial bonding. - Mechanical: tensile strength up to 10.41 MPa (+273%), modulus up to 42.61 MPa (+43.5\times), elongation max 444% at 10 wt%. - Thermal: Tg decreased with ACN's addition due to reduced hard–soft segment interactions; storage modulus at 70 °C up to 14 times higher than pure PU, indicating superior thermal-mechanical stability. 	[18]
5	CNCs from plant fiber by sulfuric acid hydrolysis	Chemical Modification: Etherification/Esterification Esterification with acryloyl chloride (AC) in dimethylformamide (DMF)/Triethylamine (TEA)	Epoxy polymer (EP)/CNCs (0.5–1.0 wt%) & EP/FCNC (M-CNCs) (0.2–1.0 wt%) via stereolithography (SLA)	<ul style="list-style-type: none"> - Unmodified CNCs: poor dispersion, phase separation in SEM, decreased mechanical integrity. - functionalized CNCs (fCNCs): covalent bonding enabled uniform dispersion, thermal stability ~370°C. - Optimal at 0.5 wt%: tensile strength \pm 1655.95 kPa (+ 30%), elongation 37% (54%), toughness 144 J/m³ (100%). - 1.0 wt% showed a performance decline due to filler crowding. 	[19]

Table 1. (Continued).

No.	Nanocellulose	Modification	Nanocomposite	Findings	Ref.
6	CNCs from cotton cellulose by sulfuric acid hydrolysis	Chemical Modification: Esterification/Esterification with 11-mercaptopentadecanoic acid	NR/CNCs & NR/M-CNCs (up to 10 wt%)	<ul style="list-style-type: none"> - Unmodified CNCs: strong phase separation, poor compatibility with NR. - M-CNCs: dual function as filler and cross-linker; improved dispersion and matrix interaction. - At 10 wt%: tensile strength ± 10.2 MPa (2.4\times), strain-to-failure 1210% (1.6\times), work-of-fracture 4.60 MJ/m³ (2.9\times). - Increased cross-link density and thermal stability. 	[10]
7	CNCs from Microcrystalline Cellulose (MCC)	Chemical Modification: Esterification/Esterification with N-(3-dimethylaminopropyl)-N'-ethylcarbodiimide hydrochloride (EDC), N-hydroxysuccinimide (NHS), and peptide coupling with hexylamine	Surfactant-free polystyrene-co-ethylhexyl acrylate (PS-co-EHA) latex with CNCs (1–3 wt%)	<ul style="list-style-type: none"> - Unmodified CNCs-COOH: sodium dodecyl sulfate (SDS)-stabilized, poor reinforcement, water uptake 35–49%, storage modulus low ($E' = 0.48$ MPa at 60 °C). - Hexyl-M-CNCs: enhanced hydrophobicity, better Pickering stabilization, water uptake ~3%, improved dispersion. - At 3 wt%: $E' = 44.5$ MPa (2 orders higher), a percolating network formed, improved mechanical and barrier properties. - Higher aspect ratio (mixed-grafted (MxG)-CNCs) led to superior reinforcement. 	[20]
8	CNCs from MCC	Chemical Modification: Grafting Surface grafting with n-octadecyl isocyanate (C18)	Poly(lactic acid) (PLA)/NR + CNCs (1–5 wt%)	<ul style="list-style-type: none"> - Unmodified CNCs: located in PLA phase, increased cold crystallization temp, E' peak at 3 wt.%, no effect on disintegration rate. - C18-g-CNCs: located in NR droplets, decreased modulus and strength, high elongation >150%, plasticizing effect, delayed biodegradation due to hydrophobicity. - PLA-g-CNCs: acted as nucleating agent, improved modulus, preserved ductility. 	[21]
9	Commercial CNCs	Chemical Modification: Grafting Homogeneous 3-step modification (<i>N,N</i> -dimethylacetamide (DMAc)/ lithium chloride (LiCl) dissolution, silanization, bio-polyol grafting)	Bio-based PU foams (1–3 wt% CNCs)	<ul style="list-style-type: none"> - Unmodified CNCs: cellulose-I structure, poor dispersion, aggregates, low reinforcement. - M-CNCs1–3: improved dispersion, better filler-matrix interaction, enhanced mechanical and thermal properties. - M-CNCs3 (RV29 polyol): compressive modulus 4.81 MPa, compressive strength 255 kPa (+424.4%), finest cellular structure, best thermal stability. - Homogeneous modification outperformed the heterogeneous method. 	[22]
10	CNCs from MCC (Alfa Aesar) by sulfuric acid hydrolysis	Chemical Modification: Grafting Functionalization with 2-ureido-4-[1H]-pyrimidinone (UPy)	Thermoplastic PU + CNCs (2.5–7.5 wt%)	<ul style="list-style-type: none"> - Unmodified CNCs: increased modulus but reduced elongation and toughness. - CNCs-UPy: strong interfacial H-bonding, enhanced dispersion, bio-inspired spider silk-like network. - Optimal at 5 wt%: tensile strength ± 46 MPa (+92%), modulus +57%, elongation 2100% (+25%), toughness +124%, improved strain-induced crystallization (SIC) and hard segment ordering. - Overloading (7.5 wt%) led to aggregation and reduced performance. - CNCs-UPy shows a higher main degradation temperature (~280 °C) than CNCs, and PU/CNCs-UPy nanocomposites exhibit slightly higher onset degradation (250–370 °C, 370–430 °C) than PU/CNCs due to hydrogen bonding between CNCs-UPy and PU. 	[23]

**Table 1:** (Continued).

No.	Nanocellulose	Modification	Nanocomposite	Findings	Ref.
11	Commercial CNCs from Tianjin Mujingling Biotechnology Co. Ltd (China)	Chemical Modification: Grafting 2,4-toluene diisocyanate (TDI), 9,10-dihydro-9-oxa-10-phosphaphhenanthrene 10-oxide (DOPO)	Shape memory polyurethane (SMPU) + CNCs/M-CNCs (1–5 wt%)	<ul style="list-style-type: none"> - Unmodified CNCs: large particle size (130.1 μm), poor dispersion, limited enhancement. - M-CNCs: reduced size (17.3 μm), uniform dispersion, improved compatibility, multifunctional (mechanical, thermal, flame retardant). - Optimal at 3 wt%: tensile \pm13 MPa (+66%), elongation 189.3% (+88%), limiting oxygen index (LOI) 23.8%, UL-94 V-2, 57% maximum peak heat release heat (HRR/PHRR) reduction, crystallinity 36.9%, shape fixity/recovery >90%. - 5 wt% caused some aggregation and reduced performance. 	[11]
12	Freeze-dried CNCs from the U.S.D.A. Forest Products Laboratory	Chemical Modification: Grafting Isophorone diisocyanate (IPDI)	PU + CNCs (1, 5 wt%)	<ul style="list-style-type: none"> - Unmodified CNCs: poor dispersion, visible aggregates, limited mechanical gain. - M-CNCs: covalent bonding with PU via pendant isocyanate groups, excellent dispersion, improved compatibility. - Optimal at 5 wt%: tensile strength \pm14 MPa (+133%) vs um-CNC, work of fracture +132%, elongation maintained (160–190%), improved thermal stability. 	[12]
13	Celluforce NCC	Chemical Modification: Grafting <i>n</i> -Tetradecenylsuccinic anhydride (TDSA)	Poly(styrene)-block-poly(isoprene)-block-poly(styrene) (SIS) thermoplastic elastomer (TPE) + CNCs (0.7–8.0 wt%)	<ul style="list-style-type: none"> - Unmodified CNCs: poor dispersion, tensile strength 2.6 MPa, elongation 1352–1526% (vs 2786%), WCA 34°, limited compatibility. - CNCs-graft-TDSA: WCA 90°, improved dispersion, enhanced thermal stability, maximum degradation temperature (Td) max 336 °C vs 315 °C, maintained TODT (100–117 °C). - Optimal at 8 wt%: Young's modulus 4.23 MPa (+403%), storage modulus +13.7\times, toughness +1.2\times, tensile strength \pm9 MPa (+246%), excellent toughness retention. 	[24]
14	CNCs from eucalyptus	Chemical Modification: Grafting Oleyl alcohol	Biobased thermoplastic polyurethane (TPU) + CNCs (1.0–5.0 wt%)	<ul style="list-style-type: none"> - Unmodified CNCs: limited interfacial interaction, percolation threshold \sim3.9 wt%, moderate mechanical gain, poor at 5 wt% (modulus +20%, toughness reduced). - M-CNCs: improved compatibility via urethane-urethane bonding, enhanced dispersion, higher thermal stability (DTG +25 °C), tensile strength \pm3.4 MPa (+9.7% at 5 wt%), better modulus (+55% at 5 wt%), maintained elongation, toughness +35%, accelerated crystallization, processability retained. 	[2]
15	Celluforce CNCs	Chemical Modification: Silylation 3-isocyanatopropyltriethoxysilane (IPTS)	NR + CNCs/M-CNCs (2.5–20 wt%)	<ul style="list-style-type: none"> - Unmodified CNCs: poor dispersion, lower tensile strength, aggregation, WCA 29.6°, zeta potential \sim42.5 mV. - M-CNCs: WCA 74.3°, improved hydrophobicity, excellent TEM dispersion, better filler-matrix interaction. - Optimal at 10 wt%: tensile strength \pm6.7 MPa (+25%), max elongation, highest crosslink density, reduced swelling. - >10 wt% caused aggregation, viscosity increase, and reduced performance. 	[25]
16	Commercial CNCs from Nanografi, Turkey	Chemical Modification: Silylation MPS (3-methacryloxypropyl trimethoxy silane) functionalization	BMH5 acrylic adhesive + fCNCs (0.5–1.5 wt%)	<ul style="list-style-type: none"> - Unmodified CNCs: hydrophilic, poor compatibility with acrylics, onset \sim240 °C, limited reinforcement. - fCNCs40: highest grafting efficiency, superior dispersion, strong siloxane network, enhanced thermal stability (onset $>$240 °C). - Optimal at 1 wt%: peel strength 1358.7 N/m, high gel content, best adhesion balance. - 1.5 wt% gave max lap shear but risked aggregation. 	[26]

Table 1. (Continued).

No.	Nanocellulose	Modification	Nanocomposite	Findings	Ref.
17	CNCs by sulfuric acid hydrolysis	Chemical Modification: Silylation 3-isocyanatopropyltrimethoxysilane (IPMS)	Room-temperature vulcanized (RTV) silicone rubber + CNCs/ICNCs (0.5–3 wt%)	<ul style="list-style-type: none"> - Unmodified CNCs: poor compatibility with silicone, limited reinforcement, temperature at 10% weight loss (T10%) 244 °C, maximum temperature (Tmax) 268 °C. - ICNCs: improved dispersion, covalent bonding with polydimethylsiloxane (PDMS), dual role as filler and crosslinker. - Optimal at 3 wt%: tensile strength 1.45 MPa (+215%), crosslink density +84%, T10% 483 °C (+129 °C), Tmax 458 °C (+72 °C), superior to 3 wt% silicon dioxide (SiO₂) in both mechanical and thermal performance. 	[27]
18	CNCs from MCC (Linghu Xinwang Chemical Co., Ltd. Huzhou, Hubei, China) by sulfuric acid hydrolysis	Chemical Modification: Silylation 3-isocyanatopropyltrimethoxysilane (IPMS)	PDMS elastomer + CNCs/ICNCs (0.5–2.0 wt%)	<ul style="list-style-type: none"> - Unmodified CNCs: poor compatibility with PDMS, moderate thermal stability, and limited healing efficiency. - ICNCs: improved dispersion, dual role as filler and crosslinker, accelerated siloxane bond exchange. - Optimal at 2 wt%: tensile strength ±0.188 MPa (+54%), elongation +80%, shear +68.6%, T10% +73 °C, Tmax +203 °C, healing 98.33% (90 °C/24h), relaxation time decreases to 434.7s, activation energy decreases to 38 kJ/mol. 	[28]
19	Celluforce CNCs	Chemical Modification: Silylation Epoxide-functionalized silane (ES)	PU coatings + CNCs/ES-CNCs (1–5 wt%)	<ul style="list-style-type: none"> - Unmodified CNCs: hydrophilic, poor PU compatibility, aggregation, limited corrosion barrier, Tmax 312 °C, WCA 25.6°. - ES-CNCs: optimal hydrophobicity, excellent dispersion, strong interfacial adhesion, Tmax 460 °C, superior thermal barrier, WCA 72.5°. - Optimal at 3 wt%: storage modulus >1000 MPa, higher than PU/5%CNC, Tg +18 °C, intact after 25-day salt spray, best corrosion resistance and moisture exclusion. 	[29]
20	CNCs from MCC by sulfuric acid hydrolysis	Chemical Modification: Silylation γ-aminopropyltriethoxysilane (APTES)	Vegetable oil-based waterborne polyurethane (WPU) + silylated cellulose nanocrystal (SCNCs) (0.25–1.0 wt%)	<ul style="list-style-type: none"> - Unmodified CNCs: hydrophilic, poor dispersion, temperature at 5% weight loss (T5%) lower, WCA 63.2°, poor water resistance. - SCNCs-6%: WCA 80.9°, smooth surface, high amino functionality, excellent dispersion, improved thermal stability, maximum hydrophobicity. - Optimal at 0.50 wt%: tensile strength ±31.68 MPa (+80% vs WPU), CA 80.9°, T5% 230°C, best water resistance, minimal water absorption, optimal crosslinking density without aggregation. 	[30]
21	Commercial CNCs	Chemical Modification: Silylation 3-Glycidyloxypropyltrimethoxysilane (GL)	TPU + CNCs/GLCNCs (0.5–2.0 wt%)	<ul style="list-style-type: none"> - Unmodified CNCs: WCA ±86°, hydrophilic, poor TPU compatibility, increased hydrophilicity with loading, limited thermal and mechanical improvement. - GLCNCs: rougher surface, enhanced TPU compatibility, maintained thermal stability, better interfacial bonding, WCA ±92°. - Optimal at 1 wt% (film): strain 1740%, toughness 90 MJ/m², tensile strength ±18.14 MPa (+72.60%), toughness 143 MJ/m³, highest performance with orientation. 	[31]

**Table 1:** (Continued).

No.	Nanocellulose	Modification	Nanocomposite	Findings	Ref.
22	CNCs from cotton linter by sulfuric acid hydrolysis	Chemical Modification: Nucleophilic Modification Reducing-end thiol functionalization via aldime condensation	Styrene butadiene styrene (SBS) triblock elastomer + CNCs/mCNCs (10 wt%)	- Unmodified CNCs: physical hydrogen bonding only, poor filler–matrix adhesion, limited reinforcement, storage modulus ~24.5 MPa. - mCNCs: thiol groups react with SBS vinyl via thiol–ene click, covalent bonding + hydrogen bonding network, homogeneous dispersion. - Double-network (mCNCs–SBS covalent + mCNCs H-bond + SBS self-crosslinking) gave tensile strength ±28 MPa (+100%), modulus +411%, work of fracture +330%, storage modulus 34.3 MPa (+600% vs SBS). - Dynamic mechanical analysis (DMA) showed storage modulus enhancement maintained across the temperature range with restricted polymer chain motion, confirming improved thermal-mechanical stability.	[32]

3.3 Physical surface modification

This section discusses physical surface modifications of CNCs for elastomer composites, focusing on surface adsorption and plasma treatment as non-covalent strategies to improve dispersion and interfacial adhesion. These techniques aim to reduce the intrinsic hydrophilicity of CNCs and align their surface energy with more hydrophobic elastomer matrices. As summarised in Table 1, surface adsorption emerges as the most widely used approach, particularly in systems based on natural rubber and polystyrene, while plasma treatment has also been explored for PF. The following discussion outlines the underlying mechanisms and reinforcement effects achieved through these physical modification pathways.

3.3.1 Surface adsorption

Overcoming the intrinsic incompatibility between hydrophilic CNCs and hydrophobic polymer matrices requires targeted surface energy modification to improve interfacial adhesion. Nagalakshmaiah *et al.*, reported that adsorption of poly[(styrene)-co-(2-ethylhexyl acrylate)] latex onto CNCs surfaces shifted the WCA from below 50° to 97°, eliminating liquid crystalline phases and reducing interparticle hydrogen bonding. These interfacial changes enabled better integration into the polystyrene phase [16]. In elastomeric composites, Jiang *et al.*, applied CTMAB treatment, reversing the CNCs surface charge from -45.2 mV to +24.9 mV, preventing agglomeration and enhancing compatibility with non-polar natural rubber. Improved dispersion was confirmed through a reduction in Payne effect $\Delta G'$ values, indicating weaker filler networking and more uniform particle

distribution, as illustrated in the schematic representations of the surface adsorption mechanism for poly[(styrene)-co-(2-ethylhexyl acrylate)] latex and the CTMAB modification route (Figures 4 and 5) [27], [33]. Both schematics show how electrostatic attraction between the CNCs' surface and modifying agents either neutralizes or reverses surface charge, reduces hydrophilicity, and enables stable dispersion within hydrophobic matrices. Thermal stability gains were evident in both systems through surface shielding effects. The thermoplastic formulation delayed the onset of acid catalyzed degradation by masking sulfate groups, mitigating the two-step decomposition between 220 °C and 400 °C typically seen in unmodified CNCs [16], [34], [35].

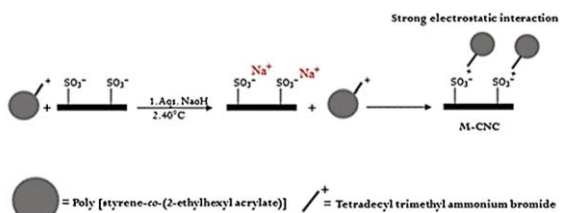


Figure 4: A schematic representation of the surface adsorption interaction between poly[(styrene)-co-(2-ethylhexyl acrylate)] latex and cellulose nanocrystals, reproduced from [16], under creative commons attribution license no. 6063040709135.

In the elastomer system, the long alkyl chains of CTMAB acted as a thermal barrier, preserving crystallinity at 69.4% compared to 72.2% for pristine nanocellulose, while also improving resistance to high temperature curing and thermal aging. Preserving crystallinity is key to retaining modulus and enabling effective stress transfer under thermal processing [17], [36].

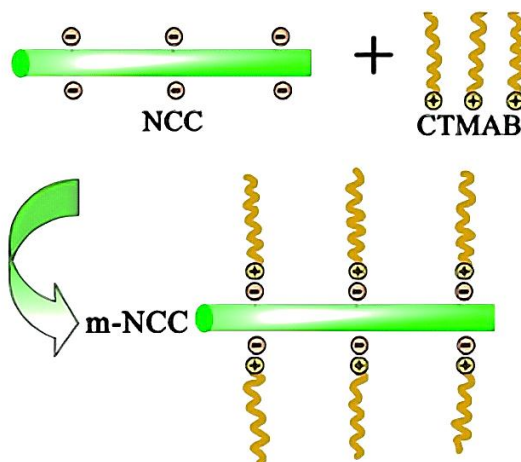


Figure 5: The modification mechanism of NCC by using CTMAB Reproduced from [17], under creative commons attribution license no. 6067060209320.

Mechanical performance results showed considerable variation. In the thermoplastic composites, the PS copolymer coating acted partially as a plasticizer, lowering the glass transition temperature and producing notable reinforcement only at higher loadings, with tensile improvements becoming significant at 10 wt% M-CNCs [16]. In contrast, the elastomer composites achieved substantial property gains at similar loadings: tensile strength increased by 132.8%, elongation by 20%, and tear strength by 66.1% over the unmodified control. Dynamic mechanical analysis revealed reduced $\tan \delta$ values in the glass transition region, supporting the constrained polymer chain model in which immobilized chains near filler surfaces enhance modulus, elasticity, and durability [17], [37].

Surface adsorption offers a simple and practical route to tailor CNCs' surfaces for elastomer reinforcement, primarily by reducing hydrogen bonding and agglomeration, thereby enabling better dispersion in hydrophobic matrices. This improved distribution enhances interfacial compatibility, increases thermal stability through shielding effects, and preserves CNCs' crystallinity, thereby supporting efficient stress transfer during curing. At moderate filler loadings, these benefits are reflected in improved mechanical performance, with notable increases in tensile strength, elongation, and tear resistance. However, the approach remains limited by its dependence on non-covalent interactions, which may result in desorption under elevated temperatures or prolonged service, which reduce long-term durability.

Stress transfer efficiency is inherently weaker than in covalent modifications, and plasticisation effects may occur in some systems, particularly at lower filler contents where reinforcement is often negligible. While attractive for its simplicity and low cost, surface adsorption is less reliable for industrial-scale elastomer applications compared with more robust covalent modification strategies.

Validation of these interfacial improvements has been consistently demonstrated in the literature through microscopic and rheological analyses. For instance, SEM and TEM imaging revealed smoother, more homogeneous dispersion of modified CNCs within elastomer matrices, confirming the suppression of agglomeration and improved phase compatibility compared to unmodified CNCs [10]–[12]. The DMA further supported these morphological findings by showing increased G' and reduced loss tangent ($\tan \delta$), indicative of restricted chain mobility and enhanced filler–matrix adhesion [11], [23], [32]. Moreover, Payne effect studies conducted by Jiang *et al.*, demonstrated a marked reduction in $\Delta G'$, signifying diminished filler–filler networking and more efficient stress transfer across the matrix–filler interface. These multi-technique validations collectively confirm that surface adsorption not only improves dispersion uniformity but also translates into measurable mechanical reinforcement and enhanced viscoelastic stability within elastomer systems.

3.3.2 Plasma treatment

Plasma induced polymerization using trans- β -farnesene effectively transformed the surface chemistry of CNCs, increasing the carbon to oxygen ratio and enhancing hydrophobicity, thereby improving interfacial affinity with polyfarnesene. The amorphous polymer coating deposited during treatment slightly reduced crystallinity from 72.3% to 69.9%, a change attributed to surface coating rather than structural degradation, indicating that the crystalline core remained intact, as highlighted by Magaña *et al.* [3]. This aligns with surface chemistry modification theory, where functional layers improve compatibility without compromising intrinsic stiffness. The *in situ* polymerization approach also promoted superior nanoparticle dispersion compared to conventional compounding, consistent with coordination polymerization theory, though still sensitive to hydroxyl group reactivity on CNCs surfaces [3].



Thermal stability profiles from thermogravimetric analysis showed minimal differences between pristine and M-CNCs, with degradation transitions near 250 °C (glycosidic bond cleavage) and 300 °C (secondary cellulose breakdown) remaining unchanged, confirming that the coating quantity was insufficient to act as a thermal barrier. Nonetheless, reduced moisture loss below 100 °C in M-CNCs reflected greater hydrophobic character, supporting the principle that hydrophobic surface functionalization reduces water uptake and improves interfacial bonding in non-polar matrices [3].

Through increased storage modulus with M-CNCs addition, mechanical reinforcement was evident and rheological analysis revealed a percolation threshold at 1.5 wt%. At this point, CNCs particles formed a continuous network, restricting chain reptation and enhancing stress transfer, a behavior predicted by percolation theory and tube model theory, where filler connectivity shifts viscoelastic response toward a solid-like regime. The storage modulus followed a fractal scaling relation ($G' \sim \phi^3$), with a higher exponent for M-CNCs composites, indicating a stronger influence on microstructural organization and frequency dependence. At higher loadings (3–5 wt%), partial percolation coexisted with agglomeration, yielding tunable viscoelastic properties but underscoring the processing and performance trade off common in nanoparticle reinforced elastomers [3], [38].

Plasma treatment modifies CNCs by depositing a thin, hydrophobic polymer layer that lowers surface energy and improves compatibility with non-polar elastomers. This coating enhances dispersion and reduces moisture uptake, while only slightly diminishing the nanocrystals' crystallinity, thereby preserving their inherent stiffness. Improved dispersion enables the formation of continuous filler networks at moderate loadings, which in turn raises the storage modulus and strengthens the overall mechanical reinforcement. Nevertheless, plasma treatment has notable drawbacks. The thermal stability of the M-CNCs remains largely unchanged, since the thin coating does not provide a strong thermal barrier. Performance gains are sensitive to filler concentration: excessive loading can cause agglomeration, which undermines dispersion and reduces mechanical benefits. Moreover, the process requires specialised equipment and careful control of coating thickness; scaling it up for industrial use while maintaining uniform coverage and preventing aggregation poses a

challenge. Thus, while plasma treatment offers an environmentally friendly way to enhance compatibility and mechanical performance, its limited thermal improvement and scaling difficulties mean it is best viewed as a complementary technique rather than a standalone solution.

The results presented in Table 1 clearly demonstrate that the efficiency of CNCs reinforcement in elastomer composites is highly dependent on filler concentration. While low-to-moderate CNCs contents typically enhance tensile strength, modulus, and interfacial adhesion due to improved stress transfer, excessive filler loadings tend to have the opposite effect. High CNCs concentrations often promote interparticle hydrogen bonding, leading to agglomeration and poor dispersion within the elastomer matrix [2], [11], [14].

This behavior is consistently reported across various systems. For example, in NR/M-CNCs composites, the mechanical properties improved up to 10 phr, but further addition (15–20 phr) caused deterioration due to filler aggregation and phase separation [3], [9]. Similarly, epoxy, polyurethane, and shape-memory PU nanocomposites exhibited performance declines beyond their optimal loading range of 3–10 wt% [11], [12], [14]. Such agglomeration restricts polymer chain mobility, reduces interfacial stress transfer efficiency, and acts as a localized stress concentrator, resulting in decreased elongation at break and toughness despite increases in stiffness or modulus [2], [10], [12].

Therefore, the optimal reinforcement balance is achieved when CNCs dispersion and polymer interfacial bonding are maximized without exceeding the percolation threshold. In most elastomer matrices reviewed here, this range lies between 0.5 and 10 wt%, depending on the modification chemistry and matrix compatibility [9], [11], [14]. Within this range, CNCs form an interconnected yet flexible network that enhances mechanical and thermal properties while preserving the inherent extensibility of the elastomer.

3.4 Chemical modification

Chemical surface modification provides a direct means to tailor CNCs for use in elastomer composites. In this approach, covalent reactions such as etherification/esterification, grafting, silylation, and nucleophilic modification are used to adjust CNCs' polarity and enhance compatibility with hydrophobic matrices. Through the introduction of functional

groups, these modifications help uniform dispersion and stronger filler–matrix interactions. As highlighted in Table 1, the most frequently reported strategies are silylation and grafting, applied predominantly in polyurethane systems of various types, with natural rubber also appearing frequently as a recurring matrix. The following sections discuss how these chemical modifications affect interfacial interactions and enhance both the mechanical and thermal performance of elastomer composites.

3.4.1 Etherification/Esterification

Chemical surface modification via etherification or esterification has been proven to markedly enhance CNCs' performance across hydrophobic matrices such as PU, elastic polymers (EP), NR, and latex templated systems. This is done by substituting hydroxyl groups with less polar functionalities, which lowers surface polarity, strengthens interfacial bonding, and improves dispersion stability. These modifications directly address the two main limitations of unmodified CNCs, namely high hydrophilicity and agglomeration in nonpolar media, effects predicted by surface energy balance theory, which states that lowering polar surface components increases compatibility with hydrophobic phases [18], [39].

In PU matrices, acetylation decreased the polar component of CNCs' surface energy from 29.5 to 12.7 mJ/m^2 while maintaining the dispersive component, resulting in an increase in water contact angle from 36.3° to 60.7° , which indicates enhanced hydrophobicity and matrix affinity. This is consistent with contact angle theory and confirms improved wettability in low-energy systems [40]. In contrast, unmodified CNCs precipitated in the same medium, showing poor compatibility and instability. In EP systems, Palaganas *et al.*, found that esterified CNCs covalently bonded with acrylate monomers, forming a kinetically stable dispersion maintained through steric hindrance and reduced interfacial tension, in accordance with colloidal stability and polymer compatibility theories. Unmodified CNCs in the same system sediment rapidly and lack dispersion stability [19]. In NR composites, thiol-ene functionalization allowed CNCs to act as both reinforcing agents and covalent crosslinkers, which enhance filler–matrix adhesion and promote uniform dispersion [41]. This dual function is absent in unmodified CNCs. Latex templated systems benefited from the amphiphilic nature of alkyl-functionalized CNCs, which acted as Pickering stabilizers, lowered oil–water interfacial

energy, and promoted network formation during evaporation, as explained by amphiphilic particle adsorption and excluded volume theories [42], [43].

Thermal performance consistently reflected improved interfacial interactions. In PU, Fourier Transform Infrared (FTIR) analysis showed a shift from hydrogen-bonded to free carbonyl groups, indicating reduced hydrogen bonding between hard and soft segments. Consistent with hydrogen bonding theory, this disruption lowered the glass transition temperature by increasing chain mobility. EP composites exhibited staged degradation: an initial mass loss between 150 °C and 200 °C from segmental breakdown into isocyanates, followed by decomposition near 300 °C involving carbamic acid, and a further 10% weight loss between 390 °C and 520 °C attributed to acrylate pyrolysis [18], [23]. Palaganas *et al.*, reported that these events are consistent with pyrolysis theory, which describes the sequential thermal scission of weaker chemical bonds [19]. In NR, covalent bonding restricted chain mobility, raising the glass transition and delaying degradation, in accordance with constrained chain mobility theory [10]. Latex templated composites-maintained CNCs' crystallinity post-modification, preserving thermal stability as explained by nanocomposite reinforcement theory, unlike unmodified CNCs that typically undergo crystallinity loss during processing [20].

Mechanical reinforcement was strongly influenced by network structure, filler geometry, and loading. In PU systems, acetylated CNCs formed a rigid percolating network at 8.5 wt%, equivalent to 5.4 vol%, facilitating efficient stress transfer via hydrogen bonding. This network effect aligns with percolation theory [44]. In contrast, unmodified CNCs failed to develop stable percolating structures in PU and led to poor dispersion, limiting their reinforcing potential and resulting in lower modulus values [18]. In EP matrices, the highest mechanical performance was observed at 0.5 wt% of functionalized CNCs. Palaganas *et al.*, indicated that load transfer improved due to homogeneous dispersion, but at higher concentrations, mechanical properties declined due to filler crowding and stress concentration, as predicted by filler packing theory. In comparison, EP composites with unmodified CNCs showed reduced strength and poor interfacial load transfer, largely due to their tendency to agglomerate and phase separate under similar conditions [19]. In NR composites, thiol-functionalized CNCs served both as reinforcing and crosslinking agents. This dual mechanism



significantly reduced stress softening (Mullins effect) from around 20% (typical for carbon black-filled rubber) to just 3–5%. Parambath Kanoth *et al.*, explained these results by covalent bonding between the filler and matrix, which maintains stress transfer and stiffness across repeated cycles, consistent with the Flory–Rehner equation for crosslink density. In contrast, unmodified CNCs showed limited interaction with the rubber matrix, resulting in weaker stress transfer and more pronounced softening. Latex templated systems achieved superior mechanical properties with CNCs of high aspect ratio (~65), which act as bridging fibers between matrix chains [10], [45]. Zhang *et al.*, demonstrated that mechanical deterioration occurs when the interconnected nanofiller network is disrupted, confirming the predictions of fibre composite mechanics and network integrity theory. Unmodified CNCs, with lower aspect ratios (~19) and poor dispersion, lacked the structural continuity needed to achieve similar reinforcing effects in the same matrix [20].

Etherification/esterification is a covalent modification methods that replace some of the cellulose hydroxyl groups with less polar functionalities. This transformation significantly improves CNCs' compatibility with hydrophobic elastomers: dispersion becomes much more uniform, and the resulting interfacial bonding is stronger, allowing stress to transfer more efficiently through the composite. Because the M-CNCs form covalent bonds with the matrix, they create percolating filler networks that increase stiffness, strength, and sometimes elongation, while also raising thermal resistance relative to unmodified CNCs. However, such chemical reactions are often multi-step processes carried out under harsh conditions and involving organic solvents, which raises concerns regarding processing complexity and long-term sustainability. In some systems, the modification can reduce interactions between hard and soft segments, lowering the glass-transition temperature and introducing a plasticising effect, and at high loadings, filler crowding can lead to property decline despite the chemical bonding. Overall, etherification/esterification offers durable, well dispersed reinforcement but at the cost of more complex processing and potential trade-offs in matrix dynamics.

3.4.2 Grafting

Grafting-based modification strategies have emerged as a versatile and highly effective approach for

engineering CNCs interfaces across diverse polymer systems, ranging from polyurethane and thermoplastic elastomers to natural rubber, bio-based foams, and shape memory of PU. By tailoring CNCs' surfaces through site-selective covalent bonding, phase-selective grafting, non-covalent interaction design, or hydrogen bonding modulation, these studies overcome the intrinsic incompatibility of unmodified CNCs with hydrophobic matrices [2], [11], [12], [22], [23], [46], [24].

Compatibility gains are evident in all cases. In immiscible PLA/NR blends, dual grafting with short PLA or C18 alkyl chains directed CNCs to either the PLA or NR phase, preserving ductility and enabling nucleation in PLA domains [46]. Compared to unmodified CNCs that localize at the interface and often disrupt phase continuity, grafted CNCs exhibit targeted dispersion and phase-specific integration, consistent with compatibilizer theory [47]. Site-selective IPDI grafting in polyurethane generated covalent CNCs–PU bonds, eliminating aggregates and resulting in optically isotropic, uniformly dispersed films, whereas unmodified CNCs in PU formed visible agglomerates and phase-separated domains [12]. Lee *et al.*, confirmed that hydrophobic functionalisation using TDSA increased the water contact angle from 34° (unmodified CNCs) to 90°, supported by DFT-calculated stabilisation energy of $-2.59 \text{ kcal mol}^{-1}$ arising from hydrophobic and OH–π interactions. These effects contrast with untreated CNCs in SIS matrices, which lack phase homology and exhibit poor wetting [24]. Oleyl alcohol-grafted CNCs in TPU disrupted inter-CNCs hydrogen bonding, enabling better filler–matrix interaction and shifting Tg of hard segments upward, while untreated CNCs showed lower Tg and poor matrix compatibility [2]. Disaggregation through DMAc/LiCl pretreatment was shown by Silvano *et al.*, to enhance grafting efficiency and improve dispersion when compared to the hydrogen-bonded CNCs clusters in untreated systems [22]. However, Tian *et al.*, reported that while UPy-modified CNCs benefited from quadruple hydrogen bonding at the interface, they experienced aggregation driven by interparticle supramolecular interactions, a limitation not encountered with unmodified CNCs, which disperse better electrostatically but offer weaker interfacial bonding [23].

Thermal stability improvements further distinguished grafted CNCs from their unmodified counterparts. In bio-based PU foams, Silvano *et al.*, identified three-stage degradation typical of grafted

systems: water loss (150–300 °C), urethane scission (350–450 °C), and large molecule breakdown (>450 °C), reflecting delayed decomposition relative to unmodified CNCs [22]. Girouard *et al.*, showed that site-selective IPDI grafting introduced a new degradation stage at 330 °C and masked sulfate groups, which are typically the first to degrade in unmodified CNCs (~250–270 °C) [12]. Grafting CNCs with TDSA, as observed by Lee *et al.*, raised the T_d max from 315 °C to 336 °C, attributed to the shielding of thermally labile surface groups [24]. Prataviera *et al.*, also reported a similar improvement, that oleyl alcohol modification delayed the onset of thermal degradation from 276 °C to 284 °C by reducing the availability of reactive surface sites. In comparison, earlier degradation was observed in unmodified CNCs, primarily due to the presence of unprotected sulfate ester groups [2]. Enhanced thermal resistance was achieved in UPy-modified CNCs, where quadruple hydrogen bonding and hard segment ordering contributed to increased thermal transition temperatures relative to the control PU–CNC composites [23]. Du *et al.*, further demonstrated that M-CNCs with urethane and DOPO grafts induced char formation and radical scavenging, offering multimodal protection not present in unmodified CNCs [11].

Mechanical reinforcement improved significantly following CNCs grafting, which often surpasses the performance of unmodified CNCs by considerable margins. In PLA/NR blends, Bitinis *et al.*, demonstrated that phase-selective placement of modified CNCs preserved ductility and enhanced PLA crystallinity, in stark contrast to unmodified CNCs, which disrupted the blend morphology and led to embrittlement [46]. Silvano *et al.*, reported a fivefold increase in compressive modulus and strength, reaching 4.81 MPa and 255 kPa, respectively, with these gains explained through the Gibson and Ashby cellular solid model. By comparison, foams reinforced with unmodified CNCs exhibited lower stiffness and irregular cellular structures [22]. Girouard *et al.*, achieved a 163 percent increase in tensile strength and a 132 percent rise in work of fracture using 5 wt% IPDI CNCs, with no sacrifice in elongation. Unmodified CNCs, on the other hand, caused premature fracture and reduced extensibility [12]. In a study by Lee *et al.*, grafting CNCs with TDSA led to a 403 percent increase in Young's modulus and a 13.7-fold enhancement in storage modulus at 8 wt% loading in SIS composites, far exceeding the improvements from untreated CNCs, which did not

reach the 5.9 %vol percolation threshold [24]. Prataviera *et al.*, showed that oleyl functionalised CNCs at 1 wt% improved both elongation and toughness. However, exceeding the percolation limit led to agglomeration and performance decline, a behaviour reminiscent of the brittleness observed in unmodified CNCs even at relatively low concentrations [2], [48]. Tian *et al.*, overcame the stiffness–toughness trade-off through strain-induced crystallization enabled by UPy–CNCs anchoring, a hierarchical effect not present in standard PU–CNCs systems [23]. Du *et al.*, demonstrated that 3 wt% M-CNCs in SMPU improved tensile strength by 66% and elongation by 88%, highlighting superior stress distribution via hybrid network formation capabilities absent in non-modified systems [11].

Grafting attaches polymer chains or functional groups directly onto the surface of CNCs, creating strong covalent bonds that markedly enhance their compatibility with a wide range of elastomer matrices. By tailoring the interface through site specific or phase specific grafting, these M-CNCs disperse uniformly and form robust filler–matrix networks, leading to significant gains in tensile strength, modulus, toughness and thermal stability compared with unmodified CNCs. Because the grafted chains can be designed to match the polarity and chemistry of the host polymer, grafted CNCs also preserve ductility in immiscible blends and enable higher percolation thresholds, allowing efficient stress transfer under load. However, the advantages of grafting come with notable challenges: the multistep reactions often require strong reagents and careful control to prevent over functionalisation, which can induce particle aggregation or reduce CNCs' crystallinity, and environmental concerns arise from the use of solvents and catalysts. At high filler contents, grafted particles can crowd and form stress concentrators, diminishing mechanical benefits. Overall, grafting delivers durable and tunable reinforcement but demands meticulous process optimisation to balance mechanical improvements against complexity and sustainability considerations.

3.4.3 Silylation

Silylation has emerged as one of the most precise and versatile chemical surface modification strategies for tailoring CNCs to suit various hydrophobic polymer matrices ranging from rigid PU and TPU to elastomers such as silicone and NR. This method is based on the hydrolysis of silane coupling agents into reactive



silanol groups, followed by condensation and covalent bonding with hydroxyl groups on CNCs surfaces to form Si–O–Si linkages (Figure 6). In PU matrices, Mekonnen *et al.*, employed epoxide-functionalized silane (ES) to transform CNCs from highly hydrophilic to moderately hydrophobic, reflected by a

WCA increase from 25.6° to 72.5° . This hydrophobicity shift, attributed to Si–O–Si crosslinking and epoxide ring-opening bonding, enhanced thermodynamic compatibility with the PU matrix [29].

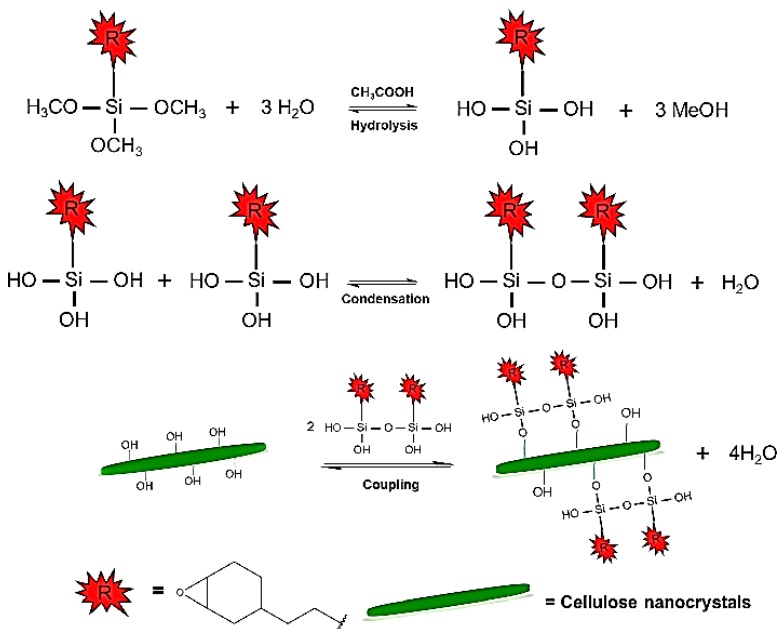


Figure 6: Illustration of epoxide-functionalized silane modification of CNCs via hydrolysis, condensation, and silanol coupling reproduced from [29], under creative commons attribution license no. 6063050796563.

In contrast, unmodified CNCs failed to disperse uniformly, causing phase separation and filler agglomeration that weakened interfacial stress transfer. Similarly, Zhang *et al.*, used APTES and found 6 wt% to be the optimal modifier level for producing smooth, uniformly coated CNCs surfaces, while overmodification at 12 wt% led to polycondensation and weaker interfacial bonding. In that system, the WCA increased from 63.2° for unmodified CNCs to 80.9° for SCNCs-6%, further evidencing the successful silane grafting and enhanced hydrophobicity. These results highlight the need to control silane condensation kinetics to preserve dispersion quality [30].

Meanwhile, glycidyltrimethoxysilane (GL) was utilised by Sun *et al.*, with successful grafting confirmed through Si–O–Si IR peaks. Enhanced hydrogen bonding and improved filler–matrix miscibility were observed, as indicated by reduced Feret diameters. A similar hydrophobicity trend was

observed, with WCA rising from approximately 86° for unmodified CNCs to around 92° for GL-CNCs, confirming surface energy modulation. Compared to unmodified CNCs–TPU composites, which showed poor filler–matrix wetting and irregular morphology, the GL-CNCs systems exhibited roundness values closer to 1.0 and stronger interfacial adhesion, as confirmed by higher hydrogen bonding index values [31].

Expanding beyond PU and TPU systems, silylation has also shown great promise in elastomeric matrices. M-CNCs with IPTS achieved a zeta potential shift from -42.5 mV to less negative values, signaling reduced surface polarity and improved interfacial energy matching [25]. Ojogbo *et al.*, reported a WCA increase from 29.6° for unmodified CNCs to 74.3° for M-CNCs, validating the transition from hydrophilic to hydrophobic surface characteristics and improved compatibility with NR matrices [25].

The reaction scheme for this surface modification is shown in Figure 7, where the isocyanate group covalently bonds with CNCs hydroxyls through carbamate formation, while the triethoxysilane group facilitates further condensation and siloxane network development, enhancing matrix compatibility. This was accompanied by increased dispersion and covalent bonding potential through carbamate linkages, confirming enhanced matrix

affinity. Further support was provided by Fan *et al.*, through the use of IPMS-treated CNCs in PDMS, where uniform coating and strong filler integration were revealed under SEM and chemical mapping. In contrast, phase discontinuities and voids were frequently observed in silicone matrices containing unmodified CNCs, attributed to poor interfacial compatibility [28].



Figure 7: Reaction scheme for CNCs surface modification using IPTS. Reproduced from [25].

Across systems, thermal stability enhancements via silylation were consistent but mechanism-specific. A shift in T_{max} from 312 °C for unmodified CNCs to 460 °C for ES-CNCs was observed, driven by the shielding effect of dense siloxane networks that act as thermal barriers and restrict chain mobility, as reported by Mekonnen *et al.* [28]. This is consistent with the barrier-layer degradation model described by Es-haghi *et al.*, and Hettegger *et al.*, where crosslinked shells hinder the diffusion of volatile decomposition products [49], [50]. Zhang *et al.*, observed a $T_{5\%}$ rise from unmodified CNCs to 230 °C due to heat insulation and mass transfer suppression [30], [51]. In contrast, Sun *et al.*, found no significant thermal gain with GL-CNCs, likely due to glycidyl silane's inherent thermal limitations, though TPU matrix integrity remained intact. These modified systems still performed thermally on par with or slightly better than unmodified CNCs-TPU composites, which often suffer from early decomposition and lower degradation onset temperatures [31].

Mechanically, the type and functionality of silane used significantly influence reinforcement. Mekonnen *et al.*, observed a T_g increase of up to 18 °C and modulus enhancement at 3 wt% ES-CNCs, confirming chain mobility restriction theory [29], [52]. In contrast, the same PU system with unmodified CNCs showed negligible T_g shifts due to weak interfacial bonding and inefficient load transfer. An 80 percent increase in tensile strength at 0.5 wt% was documented due to NH_2 -mediated crosslinking and alignment of CNCs, resembling the filament

reinforcement model [30]. However, performance was impaired at higher loadings as a result of agglomeration and percolation effects, which also limit the effectiveness of unmodified CNCs even at lower concentrations. Remarkable toughness (90 MJ/m³) and strain (1740%) were achieved in TPU-CNCs, facilitated by CNCs alignment during wet spinning and enhanced hydrogen bonding, both consistent with energy dissipation and slippage theories [31]. These values greatly surpassed those of TPU reinforced with unmodified CNCs, which typically show lower strain and reduced toughness due to rigid particle interference and insufficient matrix adhesion.

Mechanical enhancement was equally compelling in elastomeric applications. Ojogbo *et al.*, achieved a 71% increase in tensile strength at 10 wt% IPTS-CNCs in natural rubber, with further loading decreasing performance due to filler agglomeration, validating percolation threshold theory [25]. Fan *et al.*, highlighted the role of spatial control using IPMS, achieving higher elongation from 480.6% to 560.9% and increased tensile strength from 0.122 MPa to 0.188 MPa compared to traditional TEOS-treated CNCs. These enhancements exceeded those found in composites with unmodified CNCs, which often limit elongation due to the rigid behaviour of the particles [28]. Yang *et al.*, supported this by showing that modified CNCs enhanced percolating stress networks at just 2 wt% loading [27]. Fan *et al.*, further advanced this understanding by applying Maxwell models and Arrhenius analysis to show that CNCs modified with



IPMS not only enhanced composite reinforcement but also enabled dynamic mechanical behaviour through reversible Si–O–Si bond exchange [28]. This mechanism aligns with the silicon–oxygen exchange pathway [53]. These dynamic properties are not achievable with unmodified CNCs, which lack reactive surface moieties necessary for bond exchange mechanisms.

Silylation of CNCs provides a versatile platform for reinforcing elastomers: by covalently bonding organosilane molecules to CNCs, it markedly reduces surface polarity and enhances dispersion, enabling strong filler–matrix adhesion and improved stress transfer. Dense siloxane networks confer higher thermal stability, and carefully chosen silanes can raise tensile strength, modulus, and elongation while tuning viscoelastic behaviour. However, these benefits come with trade-offs. The process demands precise control over hydrolysis and condensation, uses reactive silane precursors, and may become cost intensive at scale. Beyond a certain filler loading, silanised particles agglomerate and performance declines, and some silane types offer limited thermal or mechanical gains. Hence, silylation is a powerful but nuanced strategy: its success in elastomer reinforcement hinges on matching the silane chemistry to the polymer matrix, optimising filler loading, and balancing process complexity with performance.

3.4.4 Nucleophilic modification

Nucleophilic modification of CNCs targets the reducing ends of the nanocrystals, where aldehyde groups offer unique reactivity. As demonstrated by Tao, Dufresne, and Lin, a site-selective strategy wherein thiol moieties were introduced at the reducing ends of CNCs, which enables subsequent nucleophilic addition via thiol–ene coupling in an SBS elastomer matrix. This approach preserves the unmodified hydroxyl groups on the CNC's backbone, allowing hydrogen bonding and filler network formation, while simultaneously creating covalent filler–matrix interactions through nucleophilic reaction pathways [32]. This end-specific nucleophilic grafting facilitates the formation of a multi-network structure: covalent filler–matrix bonding through UV-activated thiol–ene addition, filler–filler hydrogen bonding through preserved hydroxyls, and matrix–matrix crosslinking via UV induced SBS chain reactions. The spatially controlled reactivity enhances dispersion stability, as

evidenced by the S/M-CNCs products remaining suspended in tetrahydrofuran (THF) after centrifugation, whereas unmodified S/CNCs composites sedimented quickly. These results support previous theories of selective end-group functionalization, which leverage the electrophilic character of aldehyde termini for nucleophile-driven conjugation [54].

Thermal performance, analyzed via dynamic mechanical analysis, indicated marked improvement upon nucleophilic end-group modification. The storage modulus of S/mCNCs reached 34.3 MPa at 25 °C, which was 600% and 40% higher than pure SBS and unmodified S/CNCs, respectively. Introducing rigid nanofillers at terminal positions restricted polymer chain mobility, resulting in a higher modulus in both the glassy and rubbery regions. $\tan \delta$ values were also reduced by about 30% compared with the control, indicating greater efficiency in energy dissipation. These outcomes were not achieved in composites using unmodified CNCs, which lacked covalent bonding and exhibited inferior thermal and mechanical properties [32].

Mechanical properties were similarly enhanced. Nucleophilic functionalization enabled the S/M-CNCs composite to achieve 239% higher tensile strength, 411% higher modulus, 330% greater work of fracture, and a 7% increase in elongation at break compared to neat SBS. These combined improvements stem from the simultaneous activation of interactions between the filler and matrix, between fillers themselves, and within the matrix. Unmodified CNCs composites, by contrast, showed limited stress transfer, moderate stiffness, and reduced ductility due to agglomeration and weak adhesion. Cyclic tensile tests confirmed greater hysteresis loops in S/M-CNCs, reflecting improved energy absorption through microstructural resilience. These enhancements reflect the efficiency of nucleophilic functionalization in establishing reinforced composite architecture, supported by mechanistic frameworks such as the double network theory [32].

Nucleophilic modification of CNCs takes advantage of the reactive aldehyde groups at the reducing ends to introduce thiol functionalities, which can then form covalent bonds with elastomer chains through thiol–ene reactions. This approach preserves the crystalline structure of CNCs while enabling the creation of a multi-domain network that combines hydrogen bonding, covalent interactions, and matrix cross-linking. As a result, dispersion improves, leading to marked gains in storage modulus, tensile

strength, and toughness. However, the method is still at an early stage, as it involves complex steps, requires photochemical activation, and has only been shown in a narrow range of elastomers. At higher filler loadings or in different polymer matrices, these benefits may not be consistently achieved. Thus, nucleophilic modification shows considerable promise, but its industrial application will require further work to simplify the process, expand its scope, and ensure consistent reproducibility.

Quantitatively, the reinforcement efficiency of CNCs-based fillers can be distinguished across different modification approaches. Unmodified CNCs generally improve the tensile strength of elastomers by 30–60%, accompanied by moderate modulus enhancement of 40–80%, while changes in elongation and T_g remain limited within ± 2 °C owing to weak interfacial bonding and partial agglomeration [11], [16], [24]. In contrast, M-CNCs demonstrate markedly higher performance, with tensile strength increases of 120–400%, modulus gains of 200–600%, and elongation improvements of 20–80 %, together with T_g shifts up to 5–20 °C depending on filler chemistry and bonding density [12], [18], [22], [24], [28]. These enhancements originate from covalent coupling, improved dispersion, and effective stress transfer at the filler–matrix interface. The LCNCs, despite their simpler preparation, achieve comparable or even superior reinforcement, typically yielding 100–250% higher tensile strength and 150–400% higher modulus than the neat elastomer due to intrinsic hydrophobicity and lignin-derived thermal shielding [3], [9]. Collectively, these benchmarks confirm that both M-CNCs and LCNCs substantially outperform unmodified CNCs in mechanical and thermal reinforcement, while LCNCs additionally provide processing simplicity and sustainability advantages.

3.5 Other modification: Lignin-containing CNCs (LCNCs) and their potential for elastomers

LCNCs have recently attracted significant attention as multifunctional nanofillers for elastomer composites. In contrast to conventional CNCs that often require extensive surface modification to enhance compatibility with hydrophobic matrices, LCNCs inherently retain native lignin moieties. These moieties alter interfacial behavior, improve thermal resistance, and enhance mechanical performance. This dual-phase structure, consisting of crystalline cellulose cores and amorphous lignin domains, provides a hybrid morphology that improves

dispersion, interfacial adhesion, and thermal resistance. These three properties are critical in addressing the limitations commonly observed with unmodified CNCs [55].

One of the key advantages of LCNCs lies in their improved surface hydrophobicity. LCNCs extracted from oil palm empty fruit bunches exhibited a WCA of 75.1°, which is substantially higher than the 30 to 45° range typically recorded for unmodified CNCs [55]. This value is on par with or even higher than those obtained through esterification or surfactant-based modifications. The increased hydrophobicity is attributed to the presence of nonpolar aromatic and aliphatic groups in lignin that reduce the polarity mismatch with elastomer matrices. According to Young's equation and interfacial energy theory, improving surface energy alignment between filler and matrix enhances wetting, minimizes interfacial tension, and promotes uniform dispersion [55].

The colloidal stability is another domain where LCNCs show improved performance. Teh *et al.*, measured a zeta potential of -56.9 mV for LCNCs, exceeding the typical -30 to -40 mV range observed in sulfuric-acid-derived CNCs. This higher surface charge improves electrostatic stabilization in aqueous and latex-based systems, allowing uniform dispersion without surfactant assistance. Modified CNCs often require additional surface grafts or cationic agents to achieve comparable stability, suggesting that LCNCs offer a more direct route to effective nanofiller dispersion [55].

LCNCs also significantly enhanced thermal stability. Whereas unmodified CNCs generally begin to degrade between 200 and 250 °C, LCNCs have demonstrated degradation onset temperatures ranging from 285 to 310 °C. This performance is comparable to silane- or graft-modified CNCs, in which dense surface networks contribute to thermal shielding. In the case of LCNCs, the aromatic and condensed structure of lignin acts as a thermal barrier that delays decomposition. This characteristic makes LCNCs suitable for use in elastomer systems that undergo high-temperature curing, such as sulfur vulcanization [56], [57].

Though most LCNCs research has focused on thermoplastic matrices, their potential in elastomer reinforcement is well supported. Ouyang *et al.*, demonstrated that incorporating LCNCs into electrospun PLA mats increased tensile strength by 47.3% and Young's modulus by 60.5%. These improvements were attributed to improved dispersion and interfacial bonding. Although PLA is a



thermoplastic, the underlying stress transfer and phase interaction mechanisms are conceptually similar in elastomer matrices. This indicates that LCNCs could deliver mechanical enhancements in rubber systems through similar pathways as modified CNCs [58].

Beyond performance, LCNCs offer important sustainability advantages. Their production involves fewer chemical steps and requires lower energy input. For example, LCNCs have been produced via ball milling without chemical pretreatment [58], and isolated from corn stover using deep eutectic solvents [57]. Furthermore, Teh *et al.*, reported that producing LCNCs can lower chemical costs by about 62% and cut energy use by 80% compared with conventional CNCs synthesis. In contrast, many chemical modification methods require multiple reaction steps, rely on organic solvents, and involve lengthy purification, all of which increase costs and raise environmental concerns. By making use of agricultural waste streams, LCNCs offer a more practical route that fits well with green chemistry principles and supports circular economy goals [55].

The reproducibility of LCNCs across biomass sources is limited by inherent variability in lignin content and structure [59], which in turn affects surface chemistry, crystallinity, and interfacial properties [60]. When lignin content varies between feedstocks, LCNCs tend to show corresponding shifts in surface reactivity and colloidal stability, with trade-offs often emerging between higher lignin loading (which can decrease surface functionality available for further modification) and improved processability or lignin-derived functionality [61]. Modifications that reduce surface reactivity (e.g., effective lignin masking or selective lignin removal) can improve consistency but may reduce the opportunity for certain surface chemistries unless compensatory functionalization is introduced. Across studies, controlling feedstock composition, pretreatment, and post-processing steps is essential to approach reproducibility, and deliberate design of surface chemistries is typically needed to balance surface reactivity with stability and processability.

LCNCs offer notable advantages for elastomer reinforcement, as the residual lignin reduces polarity and enhances hydrophobicity, improving dispersion and interfacial adhesion in non-polar matrices. Their more negative zeta potential also contributes to greater colloidal stability, while lignin's aromatic structure provides a thermal shielding effect, raising degradation onset temperatures and enabling better

performance during curing. These features, together with the reduced chemical processing required for their extraction, make LCNCs effective and sustainable fillers. However, their heterogeneous surface chemistry and variable lignin content can lead to inconsistent reinforcement, creating challenges in dispersion and quality control. At higher loadings, agglomeration and reduced hydrogen bonding may hinder performance, and the need to optimize lignin retention and uniformity remains a critical challenge for wider application.

4 Benchmarking Protocol for CNCs-Based Elastomer Composites

To facilitate reproducible comparison between CNCs-based elastomer composites and industrial fillers such as carbon black and silica, a standardized benchmarking protocol is recommended. All formulations should be tested at equivalent volume fractions using identical curing conditions to ensure fair evaluation. Static mechanical properties, including tensile strength, modulus at 100% and 300%, elongation at break, tear resistance, and Shore hardness, should be determined according to ASTM D412 and D624. Dynamic mechanical analysis (DMA) over -80°C to $+150^{\circ}\text{C}$ (1 Hz, $3^{\circ}\text{C min}^{-1}$) and frequency sweeps (0.1–100 Hz) are proposed to evaluate storage and loss moduli, $\tan \delta$, and glass-transition behavior. Fatigue performance can be quantified through tension–tension cyclic tests (1–10 Hz) to construct S–N curves, complemented by fatigue crack-growth (da/dN) measurements using notched specimens. Thermal and thermo-oxidative aging should be performed at 70°C and 100°C for 24–168 h, with post-aging tensile and hardness retentions reported. Complementary analyses such as TGA, DSC, and solvent-swelling (for crosslink density) are recommended to assess structural and thermal stability. This comprehensive testing matrix provides a unified platform for benchmarking CNCs-reinforced elastomers against industrial fillers in terms of processing, mechanical integrity, dynamic response, and long-term durability.

5 Challenges

From a process standpoint, many chemical modifications involve multiple reaction steps, controlled environments (e.g., moisture free conditions for silanes, UV or click chemistry setups

for nucleophilic grafting) and stringent purification protocols. While surface adsorption is low cost and scalable, its non-covalent nature affords only short-term benefits; plasma polymerisation requires specialised equipment and careful control of coating thickness. For grafting and silylation, expensive reagents, long reaction times and solvent recycling increase operational complexity. These factors elevate processing costs and may compromise the economic viability of CNCs modified elastomers on an industrial scale.

The cost-benefit balance is further complicated by filler loading and performance trade-offs. High filler contents often needed to achieve percolation can cause agglomeration and increased viscosity, complicating compounding and extrusion. Conversely, low filler levels may not justify the cost of modification if mechanical improvements are marginal. Similarly, while LCNCs circumvent some chemical processing, heterogeneity in lignin content and batch to batch variability hinder consistent performance and quality control.

At the industrial scale, integration into existing elastomer manufacturing workflows (mixing, vulcanisation, extrusion and curing) demands robust, reproducible modifications that do not introduce contamination or disrupt rheology. Many demonstrations remain at laboratory scale; process scaling must consider larger reaction volumes, heat and mass transfer limitations, reagent recovery and environmental compliance. Furthermore, supply chains for M-CNCs, reagents and waste management need to be cost-competitive with conventional fillers such as carbon black and silica.

6 Future Perspectives

To move laboratory advances toward industrial adoption, future work should prioritize simplifying modification routes, reducing reliance on expensive or hazardous reagents, and developing continuous processes that are compatible with standard elastomer fabrication. Techno-economic and life cycle assessments are essential to evaluate true costs and environmental impacts. Greater emphasis is required on pilot scale studies that integrate M-CNCs into real compounding lines, assessing dispersion, cure kinetics, and long-term performance under service conditions. Standardising evaluation protocols and establishing quality control benchmarks for LCNCs will also be critical. Through these efforts, M-CNCs and LCNCs could transition from promising

laboratory materials to viable, sustainable fillers for high performance elastomer composites. However, realizing this potential on an industrial scale requires careful consideration of processing methods and compatibility with existing manufacturing technologies.

The industrial implementation of CNCs modification strategies depends critically on their compatibility with continuous or solvent-free processing routes such as reactive extrusion, latex compounding, and *in situ* polymerization. Among the reviewed techniques, physical adsorption and silylation appear most amenable to such scalable processing. Surface adsorption using quaternary ammonium surfactants (e.g., CTMAB, TTAB) has been successfully integrated into latex compounding lines for natural rubber and styrene–butadiene systems, achieving uniform dispersion and improved interfacial bonding under pilot-scale slurry conditions exceeding one kilogram. Likewise, silylation can be adapted to reactive extrusion or melt-compounding operations, in which hydrolyzed silane coupling agents react with CNCs hydroxyl groups to form Si–O–Si linkages during mixing. Studies by Mekonnen *et al.*, and Fan *et al.*, demonstrated reproducible dispersion and mechanical enhancement at multi-hundred-gram to kilogram scales, confirming its potential for continuous manufacturing.

In contrast, grafting and nucleophilic modification routes, although offering excellent interfacial control, generally rely on multi-step, solvent-intensive reactions in media such as DMAc/LiCl or DMF, which limit compatibility with large-scale continuous operations. Recent research into reactive extrusion employing bio-based diisocyanates or solid-state grafting has begun to address these limitations but remains confined to the laboratory scale. Consequently, from a technological readiness perspective, physical adsorption and silylation currently represent the most promising and scalable modification pathways for the industrial production of CNCs elastomer composites. However, while these methods show potential in improving material performance, their economic and environmental implications have yet to be comprehensively evaluated, which limits their industrial adoption.

Despite extensive research on the mechanical and thermal reinforcement performance of M-CNCs and LCNCs, few studies have incorporated quantitative life-cycle or cost-benefit assessments relative to conventional fillers such as carbon black



and silica. To address this gap, a conceptual framework is proposed integrating life cycle assessment (LCA) and cost–benefit analysis (CBA). The LCA component should consider resource extraction, feedstock preparation, chemical modification, energy consumption during composite fabrication, product durability, and end-of-life options such as biodegradation or recovery. The CBA dimension would include processing cost, reagent usage, scalability, and economic returns from enhanced product lifetime or reduced environmental penalties. Coupling both analyses would enable a holistic comparison of sustainability performance across filler types, facilitating the transition from laboratory development to industrial implementation of CNCs-based elastomer composites.

7 Conclusions

This review has elucidated the current advancements in surface modification strategies of CNCs for elastomer reinforcement. Both physical and chemical modification techniques have proven effective in mitigating the intrinsic hydrophilic–hydrophobic incompatibility between CNCs and elastomer matrices, thereby improving dispersion, interfacial adhesion, and stress transfer efficiency. Physical approaches such as surface adsorption and plasma treatment provide simple and scalable pathways to enhance compatibility, whereas chemical strategies including etherification/esterification, grafting, silylation, and nucleophilic modification afford stronger covalent linkages and greater thermal–mechanical stability. Moreover, LCNCs present a sustainable and cost-effective alternative by combining inherent hydrophobicity with simplified processing, aligning with current trends in bio-based and eco-efficient material design.

Despite these promising developments, large-scale implementation of CNCs- and LCNCs-based elastomer composites remains constrained by process complexity, limited reproducibility, and economic considerations. Future investigations should therefore emphasize scalable modification routes, life-cycle assessment, and standardized benchmarking protocols to ensure reliable comparison with conventional fillers. Addressing these aspects will be crucial to bridge the gap between laboratory research and industrial application, enabling the broader adoption of CNCs- and LCNCs-reinforced elastomers as sustainable, high-performance materials.

Author Contributions

M.T.A.F.: conceptualization, investigation, writing original draft, data analysis, research design, and visualization; K.N.M.A.: investigation, research idea, methodology, reviewing and editing.

Conflicts of Interest

The authors declare no conflict of interest.

References

- [1] A. C. Pandian, M. Thirumurugan, J. S. Parveen, and G. Rajesh, “3D fused deposition modelling of PLA/PBAT nanocomposites reinforced with GnP: Mechanical and thermal characterizations,” *Journal of Elastomers & Plastics*, 2025, doi: 10.1177/00952443251339798.
- [2] R. Prataviera, E. Pollet, R. E. S. Bretas, L. Avérous, and A. A. Lucas, “Nanocomposites based on renewable thermoplastic polyurethane and chemically modified cellulose nanocrystals with improved mechanical properties,” *Journal of Applied Polymer Science*, vol. 135, no. 45, 2018, Art. no. 46736, doi: 10.1002/app.46736.
- [3] I. Magaña et al., “Fully bio-based elastomer nanocomposites comprising polyfarnesene reinforced with plasma-modified cellulose nanocrystals,” *Polymers*, vol. 13, no. 16, p. 2810, 2021, doi: 10.3390/polym13162810.
- [4] W. Somphol et al., “Extraction of cellulose nanocrystals and nanofibers from rubber leaves and their impacts on natural rubber properties,” *Applied Science and Engineering Progress*, vol. 17, no. 2, 2024, Art. no. 7281, doi: 10.14416/j.asep.2023.11.010.
- [5] D. Dayanti et al., “Tuning rigid polyurethane foam with eco-friendly cellulose nanocrystals from oil palm empty fruit bunches as energy-efficient material composites for buildings,” *Applied Science and Engineering Progress*, vol. 17, no. 4, 2024, Art. no. 7544, doi: 10.14416/j.asep.2024.09.001.
- [6] D. Sonowal and K. M. Wani, “Comprehensive review of cellulose nanocrystals: Preparation, properties, modifications and applications,” *Bulletin of the National Research Centre*, vol. 49, no. 55, 2025, doi: 10.1186/s42269-025-01349-9.
- [7] S. S. Qureshi, S. Nizamuddin, J. Xu, T. Vancov,

and C. Chen, "Cellulose nanocrystals from agriculture and forestry biomass: Synthesis methods, characterization and industrial applications," *Environmental Science and Pollution Research*, vol. 31, no. 4, 2024, doi: 10.1007/s11356-024-35127-3.

[8] A. Werner, V. Schmitt, G. Sèbe, and V. Héroguez, "Synthesis of surfactant-free micro- and nanolatexes from Pickering emulsions stabilized by acetylated cellulose nanocrystals†," *Polymer Chemistry*, vol. 28, no. 39, 2017, doi: 10.1039/c7py01203a.

[9] Y. Zhang, V. Karimkhani, B. T. Makowski, G. Samaranayake, and S. J. Rowan, "Nanoemulsions and nanolatexes stabilized by hydrophobically functionalized cellulose nanocrystals," *Macromolecules*, vol. 50, no. 16, 2017, doi: 10.1021/acs.macromol.7b00982.

[10] B. P. Kanoth, M. Claudino, M. Johansson, L. A. Berglund, and Q. Zhou, "Biocomposites from natural rubber: Synergistic effects of functionalized cellulose nanocrystals as both reinforcing and cross-linking agents via free-radical thiol-ene chemistry," *ACS Applied Materials & Interfaces*, vol. 7, no. 30, 2015, doi: 10.1021/acsami.5b03115.

[11] W. Du, Z. Zhang, C. Yin, X. Ge, and L. Shi, "Preparation of shape memory polyurethane/modified cellulose nanocrystals composites with balanced comprehensive performances," *Polymers for Advanced Technologies*, vol. 32, no. 12, pp. 4710–4720, 2021, doi: 10.1002/pat.5464.

[12] N. M. Girouard, S. Xu, G. T. Schueneman, M. L. Shofner, and J. C. Meredith, "Site-selective modification of cellulose nanocrystals with isophorone diisocyanate and formation of polyurethane-CNC composites," *ACS Applied Materials & Interfaces*, vol. 8, no. 2, 2015, doi: 10.1021/acsami.5b10723.

[13] C. K. Arvinda Pandian, M. M. Dharmaraj, M. Thirumurugan, and H. Siddhi Jailani, "Basalt fabric/(3-aminopropyl) triethoxysilane modified epoxy laminates reinforced with nano-silica, OMMT and GNP: Mechanical and dynamic mechanical studies," *Polymer Bulletin*, vol. 81, no. 13, pp. 11955–11974, 2024, doi: 10.1007/s00289-024-05261-6.

[14] F. Coccia et al., "Chemically functionalized cellulose nanocrystals as reactive filler in bio-based polyurethane foams," *Polymers*, vol. 13, no. 15, 2021, doi: 10.3390/polym13152556.

[15] M. J. Page et al., "The PRISMA 2020 statement: An updated guideline for reporting systematic reviews," *BMJ*, vol. 372, p. 71, 2021, doi: 10.1136/bmj.n71.

[16] M. Nagalakshmaiah, O. Nechyporchuk, N. El Kissi, and A. Dufresne, "Melt extrusion of polystyrene reinforced with cellulose nanocrystals modified using poly[(styrene)-co-(2-ethylhexyl acrylate)] latex particles," *European Polymer Journal*, vol. 91, pp. 297–306, 2017, doi: 10.1016/j.eurpolymj.2017.04.020.

[17] W. Jiang et al., "Surface modification of nanocrystalline cellulose and its application in natural rubber composites," *Journal of Applied Polymer Science*, vol. 137, no. 39, pp. 1–10, 2020, doi: 10.1002/app.49163.

[18] S. Lin et al., "Structure and mechanical properties of new biomass-based nanocomposite: Castor oil-based polyurethane reinforced with acetylated cellulose nanocrystal," *Carbohydrate Polymers*, vol. 95, no. 1, pp. 91–99, 2013, doi: 10.1016/j.carbpol.2013.02.023.

[19] N. B. Palaganas, J. O. Palaganas, S. H. Z. Doroteo, and J. C. Millare, "Covalently functionalized cellulose nanocrystal-reinforced photocurable thermosetting elastomer for 3D printing application," *Additive Manufacturing*, vol. 61, 2023, Art. no. 103295, doi: 10.1016/j.addma.2022.103295.

[20] Y. Zhang, H. Yang, N. Naren, and S. J. Rowan, "Surfactant-free latex nanocomposites stabilized and reinforced by hydrophobically functionalized cellulose nanocrystals," *ACS Applied Polymer Materials*, vol. 2, no. 6, pp. 2291–2302, 2020, doi: 10.1021/acsapm.0c00263.

[21] N. Bitinis et al., "Poly(lactic acid)/natural rubber/cellulose nanocrystal bionanocomposites Part I. Processing and morphology," *Carbohydrate Polymers*, vol. 96, no. 2, pp. 611–620, 2013, doi: 10.1016/j.carbpol.2013.02.068.

[22] S. Silvano et al., "Synthesis of bio-polyol-functionalized nanocrystalline celluloses as reactive / reinforcing components in bio-based polyurethane foams by homogeneous environment modification," *International Journal of Biological Macromolecules*, vol. 278, no. 4, 2024, Art. no. 135282, doi: 10.1016/j.ijbiomac.2024.135282.

[23] D. Tian et al., "High-performance polyurethane nanocomposites based on UPy-modified cellulose nanocrystals," *Carbohydrate Polymers*, vol. 219, pp. 191–200, 2019, doi:



10.1016/j.carbpol.2019.05.029.

[24] H. Lee et al., "Non-covalent interaction induces controlled reinforcement of thermoplastic elastomer composites homologously incorporated with hydrophobized cellulose nanocrystals," *Composites Part B: Engineering*, vol. 282, 2024, Art. no. 111579, doi: 10.1016/j.compositesb.2024.111579.

[25] E. Ojogbo, C. Tzoganakis, and T. H. Mekonnen, "Silane-modified cellulose nanocrystals (CNCs) based natural rubber composites," *Composites Part A: Applied Science and Manufacturing*, vol. 190, 2025, Art. no. 108632, doi: 10.1016/j.compositesa.2024.108632.

[26] S. Esmaeili and M. R. Moghbeli, "Crosslinkable latex-based acrylic adhesives containing functionalized cellulose nanocrystals (fCNCs)," *International Journal of Adhesion and Adhesives*, vol. 132, 2024, Art. no. 103700, doi: 10.1016/j.ijadhadh.2024.103700.

[27] X. Yang et al., "Mechanical reinforcement of room-temperature-vulcanized silicone rubber using modified cellulose nanocrystals as cross-linker and nanofiller," *Carbohydrate Polymers*, vol. 229, 2020, Art. no. 115509, doi: 10.1016/j.carbpol.2019.115509.

[28] X. Fan et al., "Modified cellulose nanocrystals are used to enhance the performance of self-healing siloxane elastomers," *Carbohydrate Polymers*, vol. 273, pp. 1–11, 2021, Art. No. 118528, doi: 10.1016/j.carbpol.2021.118529.

[29] T. H. Mekonnen, T. Haile, and M. Ly, "Hydrophobic functionalization of cellulose nanocrystals for enhanced corrosion resistance of polyurethane nanocomposite coatings," *Applied Surface Science*, vol. 540, 2021, Art. no. 148299, doi: 10.1016/j.apsusc.2020.148299.

[30] P. Zhang, Y. Lu, M. Fan, P. Jiang, and Y. Dong, "Modified cellulose nanocrystals enhancement to mechanical properties and water resistance of vegetable oil-based waterborne polyurethane," *Journal of Applied Polymer Science*, vol. 136, no. 47, pp. 1–8, 2019, doi: 10.1002/app.48228.

[31] X. Sun et al., "Fabrication of silane-grafted cellulose nanocrystals and their effects on the structural, thermal, mechanical, and hysteretic behavior of thermoplastic polyurethane," *International Journal of Molecular Sciences*, vol. 24, no. 5, 2023, doi: 10.3390/ijms24055036.

[32] H. Tao, A. Dufresne, and N. Lin, "Double-network formation and mechanical enhancement of reducing end-modified cellulose nanocrystals to the thermoplastic elastomer based on click reaction and bulk cross-linking," *Macromolecules*, vol. 52, no. 15, pp. 5894–5906, 2019, doi: 10.1021/acs.macromol.9b01213.

[33] J. Fröhlich, W. Niedermeier, and H. D. Luginsland, "The effect of filler-filler and filler-elastomer interaction on rubber reinforcement," *Composites Part A: Applied Science and Manufacturing*, vol. 36, no. 4, pp. 449–460, 2005, doi: 10.1016/j.compositesa.2004.10.004.

[34] M. Roman and W.T. Winter, "Effect of sulfate groups from sulfuric acid hydrolysis on the thermal degradation behavior of bacterial cellulose," *Biomacromolecules*, vol. 5, no. 5, pp. 1671–1677, 2004, doi: 10.1021/bm034519+.

[35] N. Lin and A. Dufresne, "Surface chemistry, morphological analysis and properties of cellulose nanocrystals with gradient sulfation degrees," *Nanoscale*, vol. 6, no. 10, pp. 5384–5393, 2014, doi: 10.1039/c3nr06761k.

[36] A. E. Krauklis et al., "Dissolution kinetics of R-glass fibres: Influence of water acidity, temperature, and stress corrosion," *Fibers*, vol. 7, no. 3, pp. 1–18, 2019, doi: 10.3390/FIB7030022.

[37] E. O. Ogunsona, P. Panchal, and T. H. Mekonnen, "Surface grafting of acrylonitrile butadiene rubber onto cellulose nanocrystals for nanocomposite applications," *Composites Science and Technology*, vol. 184, 2019, Art. no. 107884, doi: 10.1016/j.compscitech.2019.107884.

[38] A. Zohrevand, A. Ajji, and F. Mighri, "Relationship between rheological and electrical percolation in a polymer nanocomposite with semiconductor inclusions," *Rheologica Acta*, vol. 53, no. 3, pp. 235–254, 2014, doi: 10.1007/s00397-013-0750-2.

[39] D. K. Owens and R. C. Wendt, "Estimation of the surface free energy of polymers," *Journal of applied polymer science*, vol. 13, no. 8, pp. 1741–1747, 1969, doi: 10.1002/app.1969.070130815.

[40] P. Fabbri, G. Champon, M. Castellano, M. N. Belgacem, and A. Gandini, "Reactions of cellulose and wood superficial hydroxy groups with organometallic compounds," *Polymer international*, vol. 53, no. 1, pp. 7–11, 2004, doi: 10.1002/pi.1396.

[41] C. E. Hoyle and C. N. Bowman, "Thiol–ene click chemistry," *Angewandte Chemie International*

Edition, vol. 49, no. 9, pp. 1540–1573, 2010, doi: 10.1002/anie.200903924.

[42] I. Kalashnikova, H. Bizot, P. Bertoncini, B. Cathala, and I. Capron, “Cellulosic nanorods of various aspect ratios for oil in water Pickering emulsions,” *Soft Matter*, vol. 9, no. 3, pp. 952–959, 2013, doi: 10.1039/C2SM26472B.

[43] A. Dufresne, “Cellulose nanomaterials as green nanoreinforcements for polymer nanocomposites,” *Philosophical Transactions of the Royal Society A: Mathematical, Physical and Engineering Sciences*, vol. 376, no. 2112, 2018, Art. no. 20170040, doi: 10.1098/rsta.2017.0040.

[44] V. Favier, H. Chanzy, and J. Cavaillé, “Polymer nanocomposites reinforced by cellulose whiskers,” *Macromolecules*, vol. 28, no. 18, pp. 6365–6367, 1995, doi: 10.1021/ma00122a053.

[45] P. J. Flory and J. Rehner Jr, “Statistical mechanics of cross-linked polymer networks II. Swelling,” *The journal of chemical physics*, vol. 11, no. 11, pp. 521–526, 1943, doi: 10.1063/1.1723792.

[46] N. Bitinis et al., “Poly(lactic acid)/natural rubber /cellulose nanocrystal bionanocomposites. Part II: Properties evaluation,” *Carbohydrate Polymers*, vol. 96, no. 2, pp. 621–627, 2013, doi: 10.1016/j.carbpol.2013.03.091.

[47] M. Yasuniwa, S. Tsubakihara, Y. Sugimoto, and C. Nakafuku, “Thermal analysis of the double-melting behavior of poly (L-lactic acid),” *Journal of Polymer Science Part B: Polymer Physics*, vol. 42, no. 1, pp. 25–32, 2004, doi: 10.1002/polb.10674.

[48] W. Bauhofer and J. Z. Kovacs, “A review and analysis of electrical percolation in carbon nanotube polymer composites,” *Composites Science and Technology*, vol. 69, no. 10, pp. 1486–1498, 2009, doi: 10.1016/j.compscitech.2008.06.018.

[49] H. Es-Haghi, S. M. Mirabedini, M. Imani, and R. R. Farnood, “Preparation and characterization of pre-silane modified ethyl cellulose-based microcapsules containing linseed oil,” *Colloids and Surfaces A: Physicochemical and Engineering Aspects*, vol. 447, pp. 71–80, 2014, doi: 10.1016/j.colsurfa.2014.01.021.

[50] H. Hettegger, I. Sumerskii, S. Sortino, A. Potthast, and T. Rosenau, “Silane meets click chemistry: towards the functionalization of wet bacterial cellulose sheets,” *ChemSusChem*, vol. 8, no. 4, pp. 680–687, 2015, doi: 10.1002/cssc.201402991.

[51] N. Salahuddin, S. A. Abo-El-Enein, A. Selim, and O. S. El-Dien, “Synthesis and characterization of polyurethane/organomontmorillonite nanocomposites,” *Applied Clay Science*, vol. 47, no. 3–4, pp. 242–248, 2010, doi: 10.1016/j.clay.2009.10.017.

[52] P. C. Ma, N. A. Siddiqui, G. Marom, and J. K. Kim, “Dispersion and functionalization of carbon nanotubes for polymer-based nanocomposites: A review,” *Composites Part A: Applied Science and Manufacturing*, vol. 41, no. 10, pp. 1345–1367, 2010, doi: 10.1016/j.compositesa.2010.07.003.

[53] W. Schmolke, N. Perner, and S. Seiffert, “Dynamically cross-linked polydimethylsiloxane networks with ambient-temperature self-healing,” *Macromolecules*, vol. 48, no. 24, pp. 8781–8788, 2015, doi: 10.1021/acs.macromol.5b01666.

[54] L. R. Arcot, M. Lundahl, O. J. Rojas, and J. Laine, “Asymmetric cellulose nanocrystals: thiolation of reducing end groups via NHS–EDC coupling,” *Cellulose*, vol. 21, no. 6, pp. 4209–4218, 2014, doi: 10.1007/s10570-014-0426-9.

[55] K. C. Teh, M. L. Foo, C. W. Ooi, and I. M. L. Chew, “Sustainable and cost-effective approach for the synthesis of lignin-containing cellulose nanocrystals from oil palm empty fruit bunch,” *Chemosphere*, vol. 267, 2021, Art. no. 129277, doi: 10.1016/j.chemosphere.2020.129277.

[56] M. Ma et al., “Lignin-containing cellulose nanocrystals/sodium alginate beads as highly effective adsorbents for cationic organic dyes,” *International Journal of Biological Macromolecules*, vol. 139, pp. 640–646, 2019, doi: 10.1016/j.ijbiomac.2019.08.022.

[57] X. Wu et al., “Corn Stover-derived nanocellulose and lignin-modified particles: Pickering emulsion stabilizers and potential quercetin sustained-release carriers,” *Food Chemistry*, vol. 465, 2025, Art. no. 142021, doi: 10.1016/j.foodchem.2024.142021.

[58] C. Ouyang et al., “Lignin-containing cellulose nanocrystals enhanced electrospun polylactic acid-based nanofibrous mats: Strengthen and toughen,” *International Journal of Biological Macromolecules*, vol. 280, 2024, Art. no. 135617, doi: 10.1016/j.ijbiomac.2024.135617.

[59] M. Li, Y. Pu, and A. J. Ragauskas, “Current understanding of the correlation of lignin structure with biomass recalcitrance,” *Frontiers in Chemistry*, vol. 4, 2016, Art. no. 45, doi:



10.3389/fchem.2016.00045.

[60] M. Xia, O. J. Valverde-Barrantes, V. Suseela, C. B. Blackwood, and N. Tharayil, “Characterizing natural variability of lignin abundance and composition in fine roots across temperate trees: A comparison of analytical methods,” *The New Phytologist*, vol. 236, no. 6, pp. 2358–2373, Dec. 2022, doi: 10.1111/nph.18515.

[61] Q. Li et al., “Discovering biomass structural determinants defining the properties of plant-derived renewable carbon fiber,” *iScience*, vol. 23, no. 8, 2020, Art. no. 101405, doi: 10.1016/j.isci.2020.101405.